Paired Neutron Detection

KaeCee Marie Terry

A senior thesis submitted to the faculty of
Brigham Young University
in partial fulfillment of the requirements for the degree of

Bachelor of Science

John E. Ellsworth, Advisor

Department of Physics and Astronomy

Brigham Young University

April 2016

ABSTRACT

Paired Neutron Detection

KaeCee Marie Terry
Department of Physics and Astronomy, BYU
Bachelor of Science

A lithium gadolinium borate capture-gated neutron detector was used, in conjunction with time of flight techniques, to determine if paired neutrons are observable within a single detector. Data was verified by analyzing the time delays between detectors, quantifying room return rates, comparing detection rates to statistical probabilities and calculating expected neutron flux. Potentially paired neutrons were detected by our system. Future work is discussed, including improvements to code and source configurations, as well as possible experiments to be conducted.

Keywords: fission, scission, neutron emission, paired neutrons, LGB

ACKNOWLEDGMENTS

I would like to thank John E. Ellsworth for allowing me to join the Laboratory Nuclear Astrophysics Research group, for his patience as I worked to understand concepts, his mentoring as I encountered difficulties and his support as I have pursued my dreams.

A special thanks to Dr. Lawrence Rees and Dr. J. Bart Czirr for their in-depth knowledge and counsel given to help fill in the gaps and validate my thinking and my project.

I would also like to thank Alec Raymond for countless hours of explaining, re-explaining, sanity checking and assisting as I worked on this project.

In addition, I would like to acknowledge the Brigham Young University Physics and Astronomy Department who provided funding, which made this project possible.

Contents

List of Figures

List of Tables

Chapter 1

Introduction

1.1 Motivation

Nuclear fission was accidentally discovered in 1938 by two nuclear chemists. They were bombarding uranium with neutrons in hopes of discovering a new, heavier element; instead, their results included two smaller, already known elements. Since then, fission has become an integral part of research, industry and national defense efforts. It is known that during fission, particles are emitted to stabilize the system, these particles may include alpha, beta and gamma radiation as well as neutrons. There are two types of neutron emission during fission—fission fragment neutrons and scission neutrons. Fission fragment neutrons are neutrons which are emitted from the smaller pieces after fission occurs. Scission neutrons are emitted from the breaking point as fission occurs. Since neutrons are identical particles they have the ability to be coupled or paired when emitted with similar momenta (Lyuboshitz & Lyuboshitz 2008). We are interested in the pairing effect of the scission neutrons because it is postulated that the properties of these paired scission neutrons can provide insights into the spatial and temporal characteristics of the nuclear fission process. Past research on scission and paired neutrons have included large arrays of detectors which are ex-

pensive and susceptible to crosstalk (Petrascu et al. 2011). Our research objective is to determine if paired neutrons are observable within a single capture-gated detector which will simultaneously alleviating issues of expense and crosstalk.

1.2 Basic Organization of Thesis

Due to the narrow focus of this research we will begin with necessary background information about fission, scission neutrons, capture-gated detectors and time of flight methods. In chapter 3, we will discuss our experimental methods, including general setup and equipment, an overview of the analytical code used to process our data, and a discussion of data verification techniques. We will conclude, in chapter 4, with a discussion of our findings and proposals of future research to be conducted.

Chapter 2

Background Information

2.1 Nuclear Fission

Nuclear fission is a quantum mechanical process in which unstable nuclei split, or fission, into smaller fragments. This fragmentation leads to lower energy states and is therefore a more favorable configuration. There are two basic types of fission, induced and spontaneous, both of which follow the same general process. This process begins with an unstable nucleus. As the nucleus deforms into an asymmetric dumbbell shape, the nuclear attraction decreases and the Coulomb repulsion increases. When the Coulomb repulsion is strong enough fission occurs and fragments of the original nucleus are accelerated away from each other. As these fragments travel, they become more spherical in shape, thereby converting potential energy to internal excitation energy. This conversion causes the ejection of particles, such as neutrons, to remove excess energy. These neutrons, emitted isotropically from the accelerating fragments, are called fission fragment (FF) neutrons [Fig.2.1a]. When the fragments initially separate, neutrons are also emitted from the rupture point. These neutrons are called scission neutrons [Fig.2.1b].

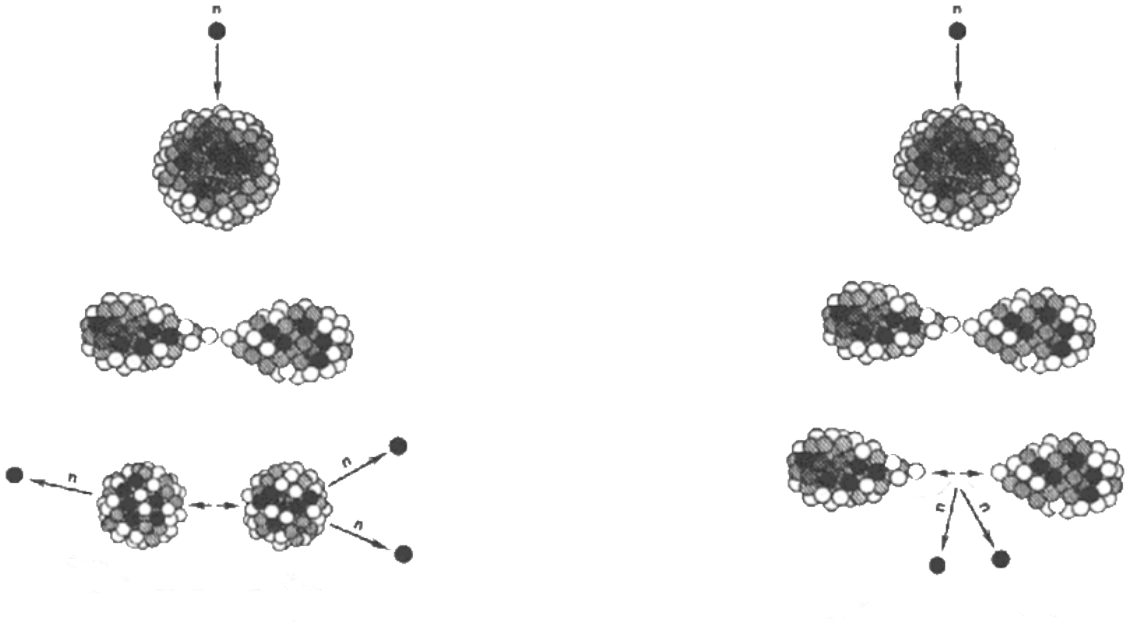

(a) FF Neutrons **(b)** Scission Neutrons

Figure 2.1 There are two basic types of neutron emission from a fission event. Fission fragment (FF) neutrons are emitted from the accelerating fragments post fission (a) and scission neutrons are emitted from the rupture point as fission occurs (b). These figures are based on Fig. 1 from The Great Soviet Encyclopedia (1979).

2.2 Scission Neutrons

Of the two types of neutron emission, scission neutrons are of the most interest to us. For many years the fission research community debated the existence and characteristics of scission neutrons (Kornilov 2015; Petrascu et al. 2011; Petrov 2005). However, it is now customary to differentiate scission neutrons from FF neutrons by their angle of emission. The exact proportion of scission neutrons to the total number of neutrons emitted is broad (1-30%), but the general consensus is that scission neutrons *do* exist (Gagarski et al. 2008; Kornilov 2015; Kornilov et al. 2001a;b; Lyuboshitz & Lyuboshitz 2008; Petrov 2005; Petrov et al. 2008; Pringle & Brooks 1975; Wagemans 1991).

Experimental differentiation confirms the existence of scission neutrons. In 1962, Harry Bowman and his colleagues at the Lawrence Radiation Laboratory in Berkeley, California performed an experiment to prove the existence of scission neutrons and provide a method to differentiate between the two mentioned types of neutrons. His setup, as shown on the left in Fig. 2.2, consisted of four detectors and a fission source. It was found, as shown in the graph on the right in Fig. 2.2, that most neutrons are found to be along the fission axis, which is established by the fission fragments. There was a small proportion of neutrons detected at the perpendicular, these are cited as scission neutrons (Bowman et al. 1962). Since 1962, similar experiments have taken place to determine the exact percentage of scission neutrons to total neutron emitted and to further certify the existence of scission neutrons (Kornilov et al. 2001a;b; Petrov 2005; Petrov et al. 2008; Wagemans 1991).

We are not only interested in the existence of scission neutrons, but we are interested in the pairing effect of scission neutrons. Within the last 12 years, a few researchers have proposed the idea of a momentum correlation between identical particles (such as low-energy neutrons from fission). This correlation effect can be used to investigate the production process of those particles, including the shape of the region and the duration of the process. The magnitude of this correlation can also be used to distinguish between FF and scission neutrons (Companis et al. 2010; Lednicky 2004; Lyuboshitz & Lyuboshitz 2008; Petrascu et al. 2011).

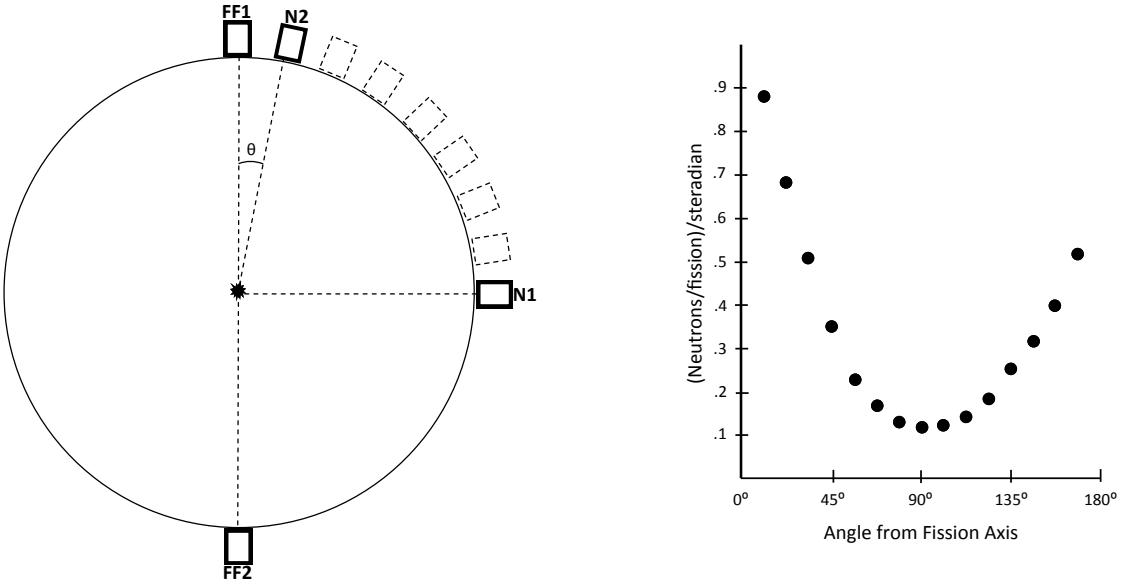

Figure 2.2 On the left is a simplified schematic of Harry Bowman's neutron detection experiment. It consisted of four detectors and a fission source. Three of these detectors were stationary; two were used to detect the fission fragments and establish the fission axis (FF1 and FF2). The third stationary detector was placed perpendicular to the fission axis and used to detect neutrons (N1). The fourth and final detector was stepped through a series of angles in 11.25 degree increments and was also used to detect neutrons (N1). On the right is a graph containing his results which consists of the number of neutrons detected versus angle from the fission axis (Bowman et al. 1962).

Another neutron-neutron correlation, which can be used to differentiate between FF and scission neutrons, is an angular correlation either between emitted neutrons and the fission axis or between the emitted neutrons themselves. This angular correlation can be used to improve and test neutron emission models (Bowman et al. 1962; Gagarski et al. 2008; Petrov 2005; Pringle & Brooks 1975).

Due to these two correlation effects, paired scission neutrons have become a prime candidate for investigating the process of neutron emission from fission. By better understanding paired scission neutrons, we will have a better understanding of the final stage of the fission process (Carjan & Rizea 2015; Petrov 2005). We will be able to probe the size, shape and duration of the neutron generation process (Lednicky 2004; Lyuboshitz & Lyuboshitz 2008; Petrascu et al. 2011), improve neutron emission models (Pringle & Brooks 1975), and increase efficiencies in nuclear fuel cycles as well as safety and security at nuclear power plants (Talou et al. 2011). In order to detect these paired neutrons, we need a proper detector.

2.3 $Li_6Gd(BO_3)_3$:Ce Capture-gated neutron detectors

Within nuclear physics, the issue of crosstalk, or multiple counting of a single event, can produce incorrect data and horrible statistics. To address this issue, a capture-gated neutron detector was developed by Dr. J. Bart Czirr, PhD with advice from John Ellsworth and Dr. Lawrence Rees, PhD. This detector was then tested by the Laboratory Nuclear Astrophysics Research and the Nuclear Research groups at Brigham Young University.

Two capture-gated neutron detectors were used during this project. The first, having a five inch diameter by four inch thick bulk of plastic scintillator, was obtained from Photogenics (Photogenics 2008). The second, was constructed during this project. Both consist of 10% by weight lithium gadolinium borate (LGB) crystals volumetrically distributed in a bulk of EJ-200 Plastic Scintillator

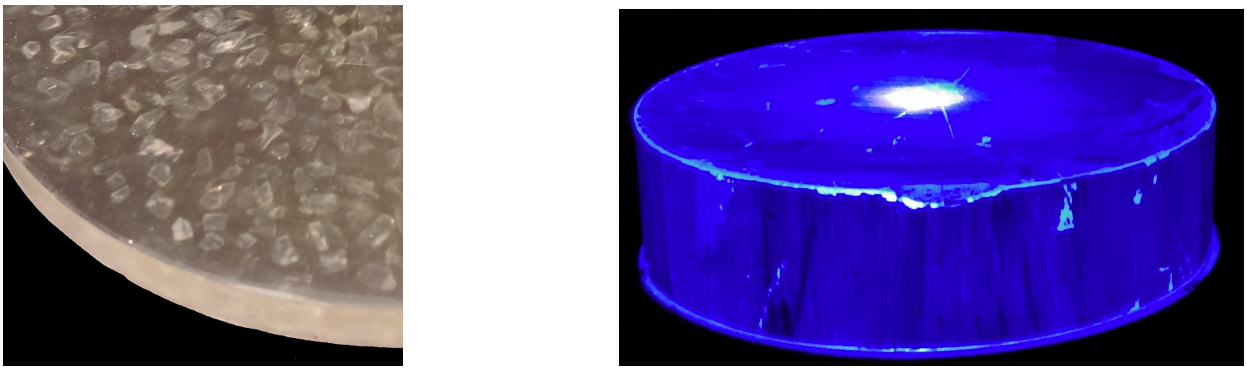

(a) LGB Crystals in Plastic Scintillator

(b) Fluorescing Plastic Scintillator

Figure 2.3 Lithium-gadolinium-borate (LGB) crystals (a) volumetrically distributed in a bulk of plastic scintillator (b). Materials used in stop detector.

[Fig. 2.3a]. The plastic is then optically coupled to a photomultiplier tube (PMT) and sealed in a light-tight metal enclosure.

Plastic scintillator is a highly hydrogenous material and acts as a moderator for and absorber of neutrons. It also fluoresces when struck by a photon [Fig. 2.3b]. As neutrons collide or recoil against protons, an exchange of energy occurs which produces a photon of light. Once a neutron loses enough energy through recoils, it can be captured or absorbed by the cerium doped LGB crystals, which independently emit light. This absorption of neutrons eliminates crosstalk. The emitted light is then detected by the PMT and converted into an analog signal for additional processing.

2.4 Time of Flight

Without some sort of reference the analog signal from a PMT would have little meaning. With the use of a time of flight facility, we are able to obtain data that has meaning and duplicability. Time of flight (ToF) is a well established method for determining the energy of neutrons and is useful for detecting valid fission events. A regular ToF event consists of a start, proton recoil, and a neutron

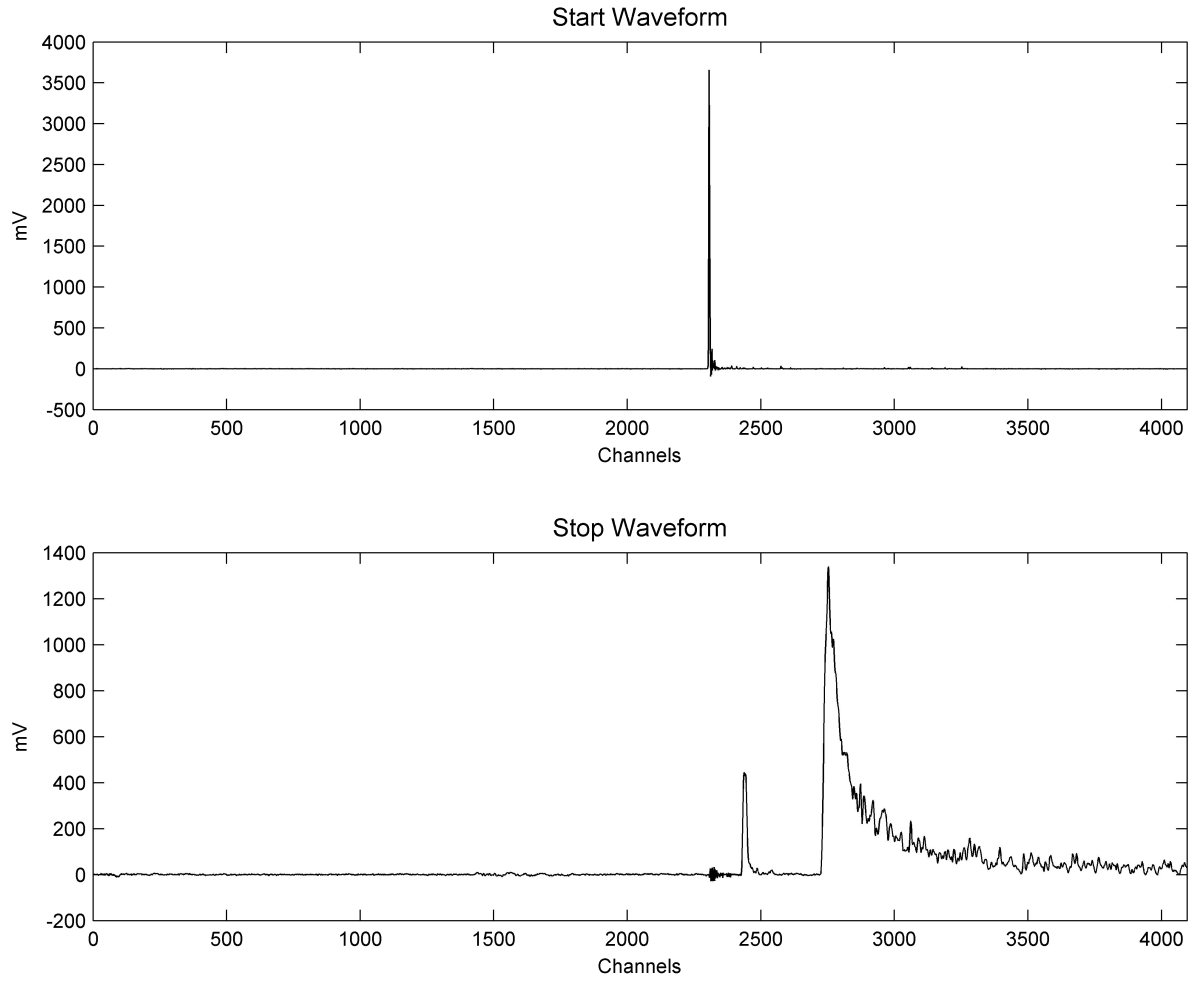

Figure 2.4 A typical time of flight event consists of a start signal or gamma flash (sharp peak on the top graph) and a stop signal (bottom graph) which consists of a proton recoil (smaller peak) and a neutron capture (larger peak with long tail). The x-axis, in channels, can be converted to time using the digitizing rates of the digitizer used in data collection.

capture [Fig. 2.4]. Our start signal comes from a gamma flash emitted from a fission event which is detected by a polyvinyl toluene (PVT) plastic scintillator optically coupled to a Hamamatsu PMT. The stop signal (proton recoil and neutron capture) comes from the LGB capture-gated detector which is placed about a meter from the fission source (Cf-252 in this case).

Chapter 3

Experimental Methods

3.1 General Setup and Equipment

Our experimental setup was developed with the specific goal of observing paired neutrons while minimizing signal loss and maximizing voltage and timing resolution. Figure 3.1 is a schematic of our data collection system (for a more detailed schematic see Appendix C).

To minimize signal loss and avoid pulse pileup both the start and stop detectors are placed at a tested distance from the fission source (20 cm for the start detector and 63 cm for the stop detector). To maximize voltage resolution we sent the signal through a timing filter amp which is used to amplify the signal, allowing us to discern smaller pulses, and clip or filter extremely large pulses (such as 30+ V pulses generally caused by muons), thereby protecting the digitizer.

Our initial data collection was performed using the Photogenics capture-gated detector which uses an Adit PMT. This detector was chosen for proof of concept—the large amount of scintillator provides more moderation for neutrons thereby increasing the probability and rate of neutron captures. One of the drawbacks of Adit PMT's is that they integrate the signal (due to limited response time) causing intricate details to be smoothed over. We were able to improve our timing resolution

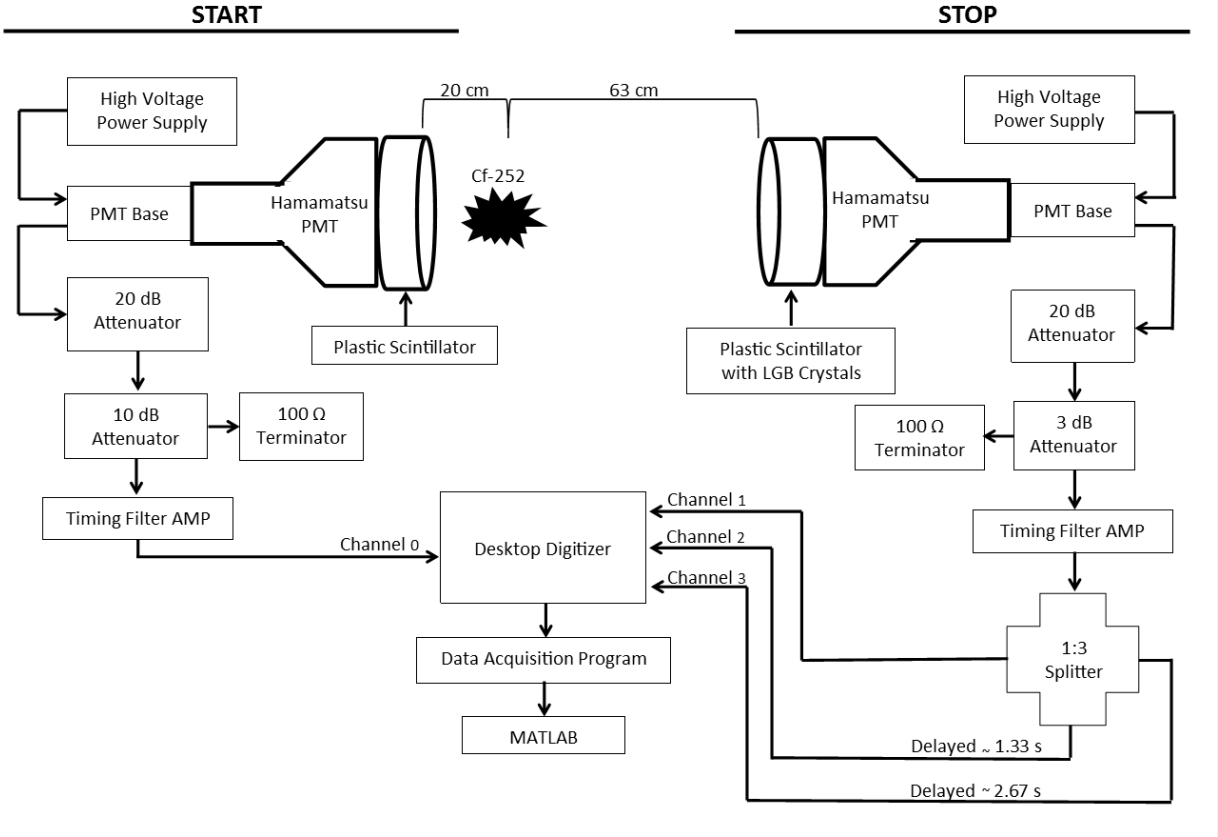

Figure 3.1 A simplified schematic of our data collection system. Both the start and stop signal come from a Hamamatsu photomultiplier tube and is sent through hardware to amplify the signal and adjust the peak-to-peak voltage ensuring a safe input signal for the desktop digitizer. Once the signal is digitized events are recorded using analytical software and then processed using MATLAB.

by switching to a Hamamatsu PMT and reducing the bulk of the plastic scintillator. As shown in Table 3.1, the rise time of a Hamamatsu PMT is about an order of magnitude faster than an Adit PMT (ET Enterprises Limited 2011). This faster response time greatly increased our timing resolution. For more information about Adit and Hamamatsu PMT's see the included datasheets in Appendix D.

Table 3.1 Comparision of physical and timing attributes of Adit and Hamamatsu Photomultiplier Tubes. Adapted from ET Enterprises *Understanding Photomultipliers* (ET Enterprises Limited 2011).

Attribute	Adit	Hamamatsu
Dynode Structure	Box & Grid	Linear Focus
No. of Stages	10	14
Transit Time (ns)	50-80	22-55
Transit Time Jitter (ns)	4.2-6.4	0.5-1.2
Rise Time (ns)	12-18	1.8-2.7

To further increase our timing resolution, we split our stop signal and separated it in time. As shown in Fig. 3.2 our signal is divided by three and delayed by 1.33 ns and 2.67 ns. This was accomplished by added delay cable along two of the signal paths.

As mentioned previously, our start detector is specifically designed to detect gamma rays and consists of polyvinyl toluene plastic scintillator doped with anthracene. The scintillator is approximately two inches thick with a five inch diameter and is optically coupled, using BC-630 silicone grease from Saint Gobain, to a Hamamatsu PMT. Our stop detector is designed to detect and capture neutrons and consists of a 1.25 inch thick by five inch diameter bulk of plastic scintillator with LGB crystals distributed throughout. Our stop detector is also coupled with a Hamamatsu PMT.

Once the signal is amplified and properly delayed it is sent through a desktop digitizer to our data acquisition software. Within the software we correct the dc offset of each signal and establish

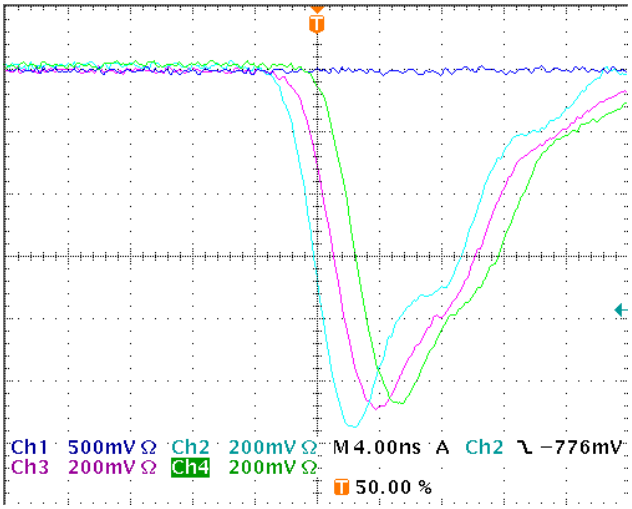

Figure 3.2 To increase timing resolution the stop signal was divided by three. Proper delay cable length was added and checked using an oscilloscope. The blue curve represents 0 ns delay, pink 1.33 ns delay and green 2.67 ns delay.

a trigger. Our trigger utilizes the distinct pulse shape of neutron captures in the LGB crystals.

All data collected is then processed using scripts composed in MATLAB, which will be discussed in Section 3.2.

3.2 Analytical Code

Herein, we will describe the general scripted procedures developed in MATLAB for sorting and selecting potentially paired neutron events.

Raw data are loaded into MATLAB one event at a time and are passed through a series of tests to ensure that (1) a start and stop signal exist above the noise level and (2) a proton recoil is present in the stop signal. Of the remaining events, the following process is undertaken to find three peaks within the stop signal and then to confirm if at least two of the peaks are neutron captures. Since the Hamamatsu PMT has high timing resolution, we begin by smoothing the stop signal to reduce the peaks in the tail of the neutron capture. Then, by using the first derivative of the smoothed

waveform, we can pick out zero-crossings and use them as markers for finding peaks within the waveform. Once a peak is found we determine the rise time of that peak and use twice the rise time to create a cut off for early area under the curve. We then compare the early area to total area under the curve to classify what kind of peak is present. Proton recoils generally have an early-to-total area ratio of 0.8-0.99 while the neutron captures have a lower ratio of 0.3-0.5. If there are two captures present, both after the proton recoil, the event is stored.

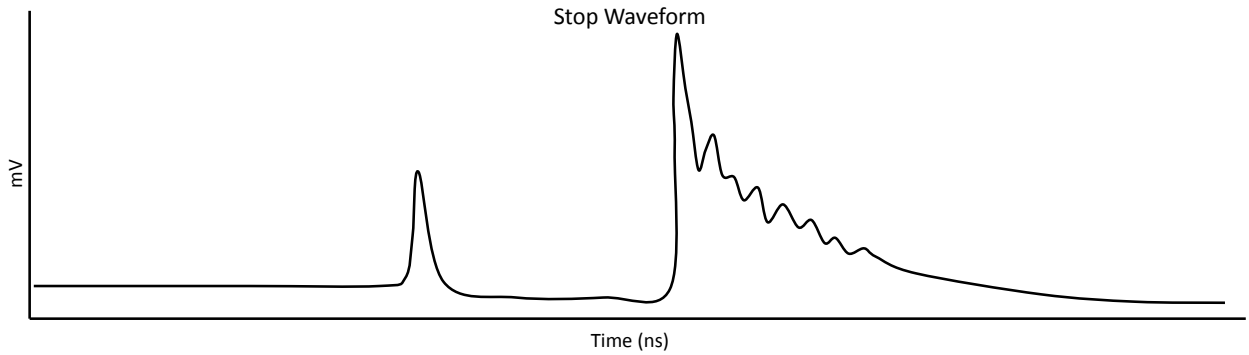

Figure 3.3 An idealistic stop waveform with a single proton recoil (first peak) and neutron capture (second peak). This is a simplified representation of a typical stop signal to demonstrate our analysis process.

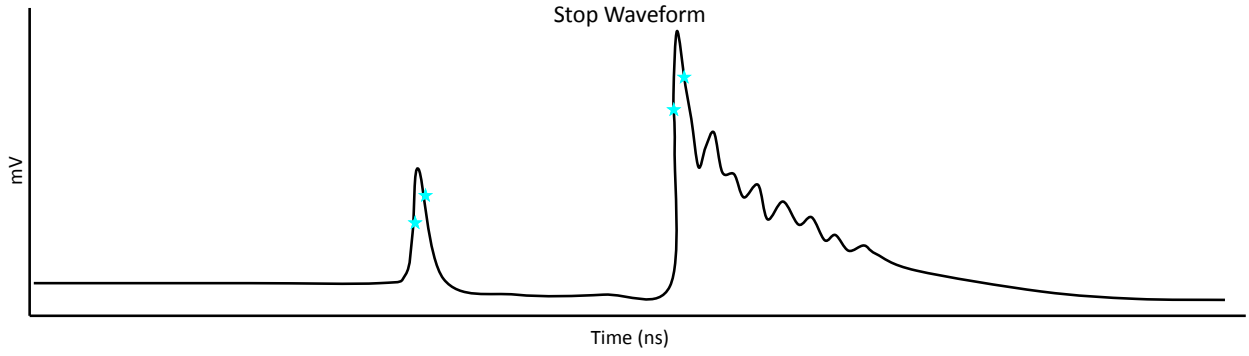

Figure 3.4 The first step in our analytical process involves finding the steepest slopes. These slopes are generally found on the rising and falling edges of a peak.

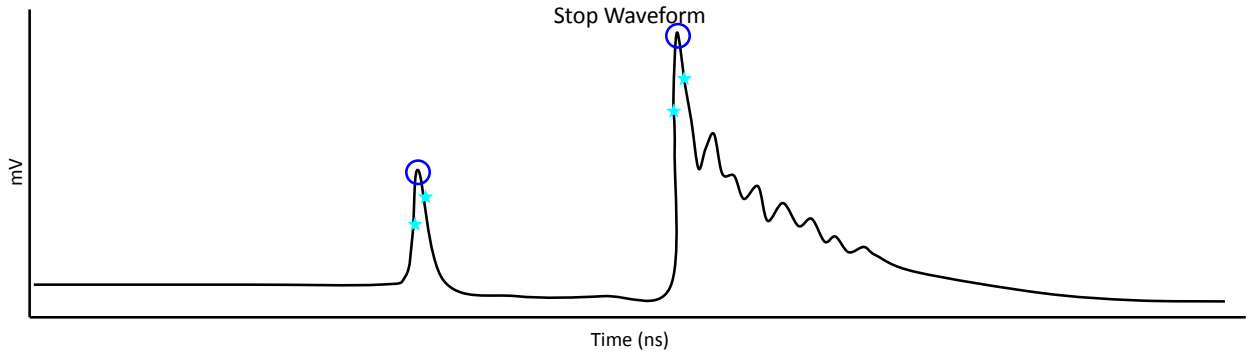

Figure 3.5 Once the steepest slopes have been found we can use these positions as outer limits between which we can find a local maximum (or a peak).

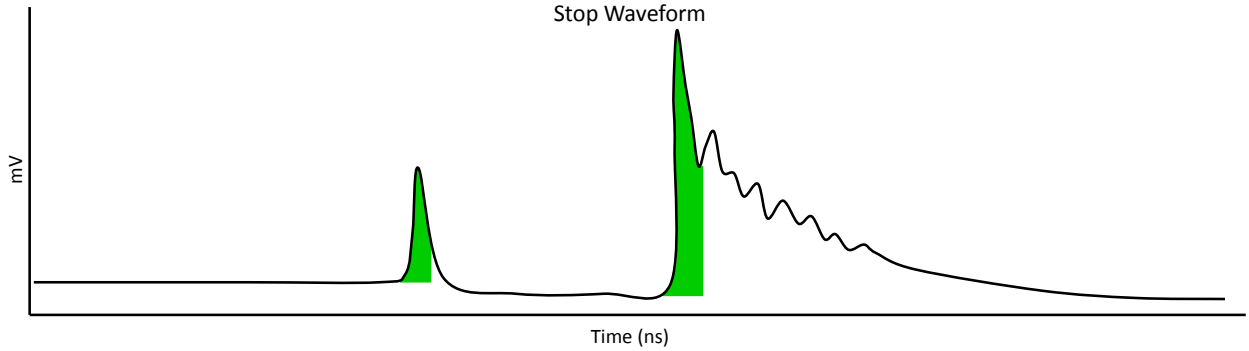

Figure 3.6 Once the peak has been found we can calculate the rise time and use this to determine a cut off for the early area.

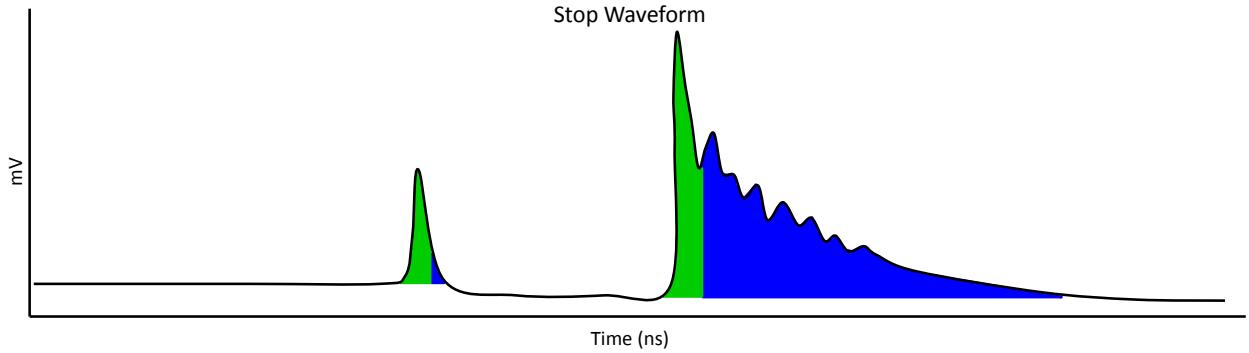

Figure 3.7 With the early area calculated we can now find the late and total area which are then used in further data processing and peak sorting.

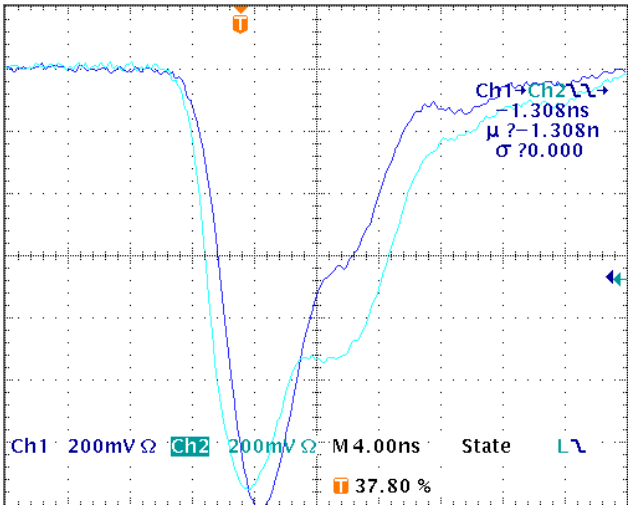

Figure 3.8 To determine the timing delay between the stop and start detectors, gamma rays from cobalt-60 can be used. The delay between the two signals is determined by comparing the falling edge at half-maximum.

3.3 Verification of Data

In order to authenticate our data and results we performed four validity tests to check delay times, room return, occurrence rates and neutron flux.

3.3.1 Timing

Since we are using the time of flight method to determine valid events and neutron energies, timing is very important. Using gamma radiation from cobalt-60, we were able to determine the timing delay between our start and stop detectors. This is accomplished by placing the start and stop detectors comparable distances from the cobalt source and using an oscilloscope to measure the time between half-maximum of both peaks. Using a 4.5 μCi cobalt-60 source we determined that there is, on average, 1.6 ns delay between our start and stop detector. This delay correction is incorporated into our analytical code ensuring that our timing for each event is correct.

3.3.2 Room Return

A fission source emits neutrons isotropically meaning that neutrons can ricochet off of the ceiling, floor or walls and into our detector. This causes our results to be skewed because the energy and time of flight of these room returned neutrons will be different than a neutron that was emitted directly into the detector. To determine the amount of room return present in our lab, we constructed a shadow bar out of paraffin wax and placed it between the source and our detector. Paraffin wax is a neutron moderator meaning it will slow down neutrons and, with sufficient depth, eliminate in-line detection. This implies that all neutrons detected are from room return and cosmic rays. After taking a data run with a comparable duration, we determined that the current room return rate in our lab is 0.5 neutrons per second.

3.3.3 Statistics of Occurrence

The next validity test performed focused on the rate of occurrence for double-recoil events and involved a comparison of actual data to simulated data created using MATLAB. We performed this test by starting with a length of time (the same length as an actual run) and randomly distributing simulated fission events within that time frame. Then we checked to see if two events were within 100 ns of each other (100 ns was the cutoff for the separation of double-recoils based on previously observed events). After performing 100 iterations of this process with 328 658 events detected in 18 hours, we found that the average number of double-recoil events per data set was 0.18. The actual data set contained five potential double-recoil events. Using our calculated rate of occurrence of 0.18 events per data set we can say that those five events are significant and not just random happenstance because the actual rate of occurrence is almost 28 times greater than the average random rate of occurrence.

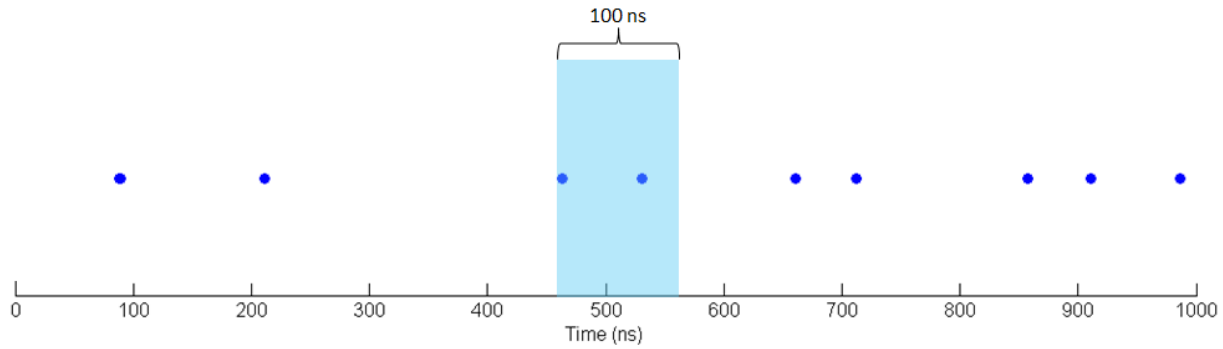

Figure 3.9 To validate the rate of occurrence of our double-recoil events we can compare our rate with the rate obtained by randomly distributing events within a given time frame.

3.3.4 Neutron Flux

Due to the isotropic emission and stochastic nature of spontaneous fission, we also confirmed our results by determining the current activity rate of our californium-252 source and the expected neutron flux through our detector.

On 1 March 2016, our source had an activity rate of

$$34.8\mu\text{Ci} = 1287\text{kBq}.$$

The probability of californium-252 to undergo spontaneous fission is 3.09% (Martin et al. 1999). We used this probability to determine the expected number of spontaneous fission events per second

$$(1287\text{kBq})\,(0.0309) = 40\text{kBq} = 40000\frac{\text{spontaneous fissions}}{\text{s}}.$$

There are, on average, 3.7 neutrons emitted per spontaneous fission (L'Annunziata 2012). Using this, we calculated the expected neutron flux

$$\left(40000\frac{\text{spontaneous fissions}}{\text{s}}\right)\left(3.7\frac{\text{neutrons}}{\text{spontaneous fissions}}\right) = 148000\frac{\text{neutrons}}{\text{s}}.$$

Since neutrons are emitted isotropically, we can model the neutron distribution over the surface of a sphere, which has a radius equal to the distance our scintillator is from the source [Fig. 3.10].

To find the number of neutrons per second which hit the face of our scintillator we multiplied the calculated neutron flux by the ratio of the surface area of our scintillator to the surface area of the overall sphere

$$\left(\frac{\text{neutrons}}{\text{s}}\right)\left(\frac{\text{Surface Area of Scintillator}}{\text{Surface Area of Sphere}}\right) = \text{detector flux}\frac{\text{neutrons}}{\text{s}}.$$

The scintillator on the stop detector has a diameter of five inches which gives us a surface area of 0.013 m^2. The face of the scintillator is placed 63 cm from the source which gives us a spherical surface area of 5 m^2. Using these two areas, we calculated the number of neutrons to hit the surface of our detector

$$\left(148000\frac{\text{neutrons}}{\text{s}}\right)\left(\frac{0.013}{5}\right) = 385\frac{\text{neutrons}}{\text{s}}.$$

No detector has 100% efficiency, therefore, we multiplied this average number of neutrons per second by the efficiency of our detector to find the expected detectable neutron flux. Using a rough comparison with the Photogenics Adit detector we estimated the efficiency of our detector to be 3.4% which gives the expected detectable neutron flux of

$$\left(385\frac{\text{neutrons}}{\text{s}}\right)(0.034) = 13\frac{\text{neutrons}}{\text{s}}.$$

By comparing our calculated neutron flux to the measured neutron flux, we can authenticate our data. If the measured rate is less than the calculated rate we know that the events which we see are valid. If the rate is greater than 13 neutrons per second, then steps can be taken to determine where the false-positives are entering the system.

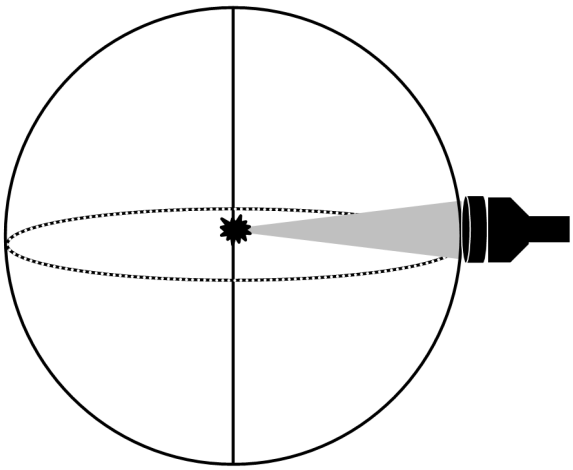

Figure 3.10 When calculating the neutron flux through a detector, the solid angle must be taken into consideration.

Chapter 4

Results

4.1 Findings

The objective of this project was to determine if paired neutrons are observable within a single capture-gated detector. We were successful in observing double-recoil and double-capture events.

Our preliminary results from the Photogenic Adit PMT demonstrated that multiple captures could be detected within the same detector. These double-capture events encouraged and propelled us forward. As we continued taking data using an Adit PMT we eventually detected a double-recoil double-capture event [Fig. 4.1]. Since the proximity of the two recoils was very close and Adit PMT's integrate or smooth the signal, we decided to switch to a Hamamatsu PMT and increased our digitizing rates in order to increase our timing resolution. With better timing resolution, we hoped to increase the separation between the two recoil peaks.

Using a Hamamatsu PMT, we were again able to detect double-recoil double-capture events [Fig. 4.2]. After 100 hours of additional data collection, we detected seven double-recoil events with valid times of flight (see Appendix A for plots of all seven events).

By analyzing these seven events, we hoped to find commonalities among double-recoil events.

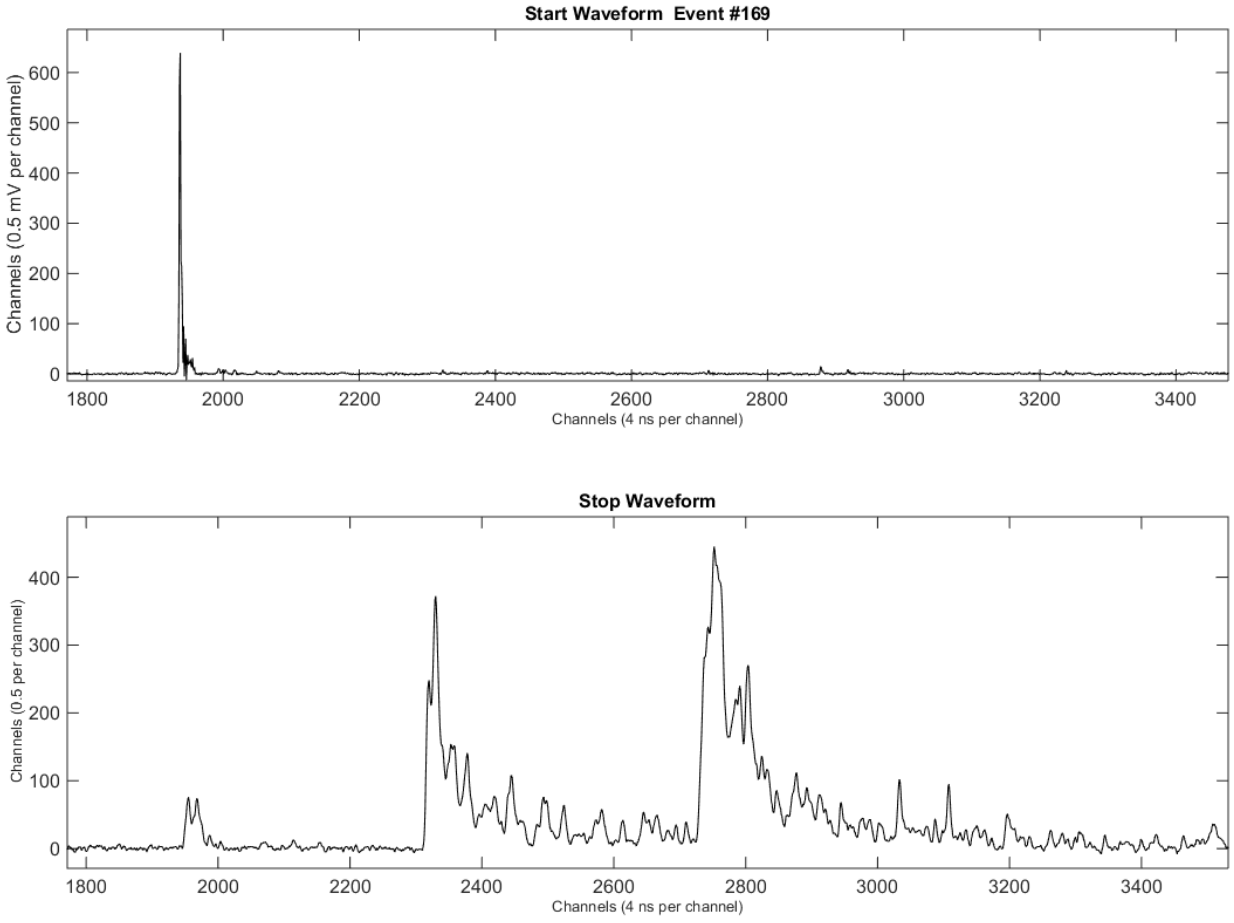

Figure 4.1 Double-recoil double-capture event detected with an Adit photomultiplier tube on 03 September 2015.

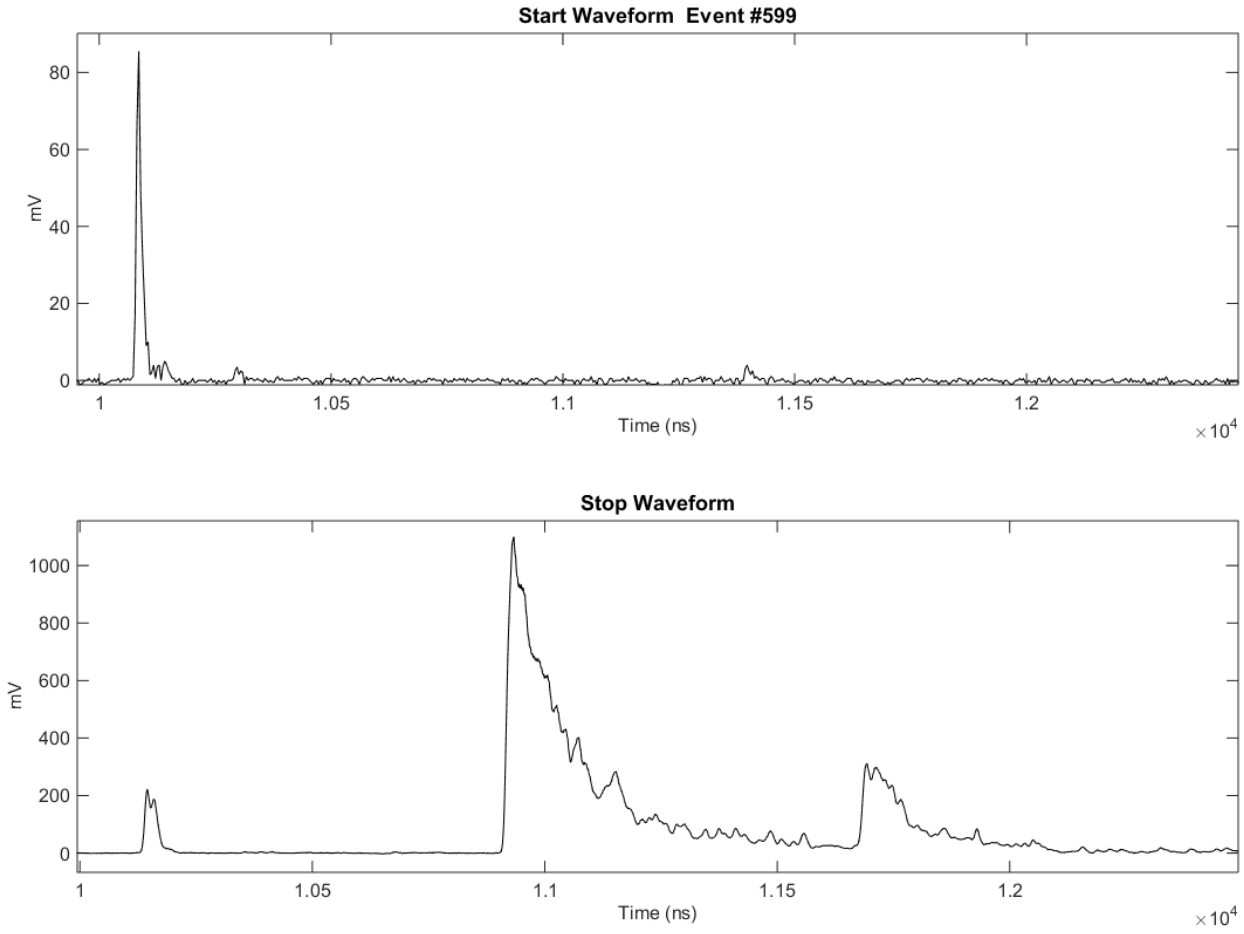

Figure 4.2 Double-recoil double-capture event detected with a Hamamatsu photomultiplier tube on 18 November 2015.

Table 4.1 contains numerical data for each double-recoil event and includes the time of flight, the time constant for the combined recoils, the width of the double-recoils, and the ratio of early area to total area. Table 4.2 includes images of the seven recoils for visual comparison.

The average time of flight for these events is 112 ns, removing the outlier (event 35) the average is 56 ns. (These times have been scaled up for comparison with a source-detector distance of one meter.) If the neutron spectrum for scission neutrons is similar to the overall neutron spectrum for californium-252 this result is encouraging. The most probable energy of neutrons emitted from californium-252 is 0.7 MeV (ToF of 86 ns) with an average energy of 2.1 MeV (Martin et al. 1999).

The consistence in the time constant and area ratio of recoils was used as part of our analysis process to sort between peak types. The peak widths are also similar except for one outlier, which suggests that this event, number 107, may not be a double-recoil, but instead a recoil and a muon. When looking at the plots in Table 4.2, most of double-recoils have a prominent first recoil and a smaller second recoil. Double-recoils which have similar heights suggest that the two neutrons struck the detector with similar energies which supports the paired neutron theory (events 231 and 35 as examples).

Another characteristic to consider when validating events is the number of captures present. Some of our double-recoil events have two captures present while others only have one. It is difficult to reject single capture events due to the nature of the recoil-capture process. Once the neutron has recoiled with a proton, it can wander within the scintillator for an indefinite amount of time before being captured in the LGB crystals. Therefore, a second capture may have occurred, but simply happened after our 16 μs collection window.

Table 4.1 Compilation of possible double-recoil events from 100 hours of data acquisition for characteristic comparison. Types include double-recoil double-capture (DR-DC) and double-recoil single capture (DR-SC).

Date	Event Number	Type	ToF (ns)	Recoil Time Constant	Recoil Peak Width	Recoil Area Ratio
2016-03-01	25	DR-DC	42.9	58.667	146.667	0.957
2016-03-04	113	DR-DC	44.4	50.667	117.333	0.963
2016-03-04	128	DR-DC	73.0	48.000	138.667	0.992
2016-03-04	107	DR-SC	36.5	60.000	568.000	0.847
2016-03-10	93	DR-DC	49.2	53.333	177.333	0.978
2016-03-10	231	DR-SC	90.5	49.333	125.333	0.987
2016-03-10	35	DR-DC	449.2	53.333	138.667	0.977

Table 4.2 Compilation of double-recoils from 100 hours of data acquisition.

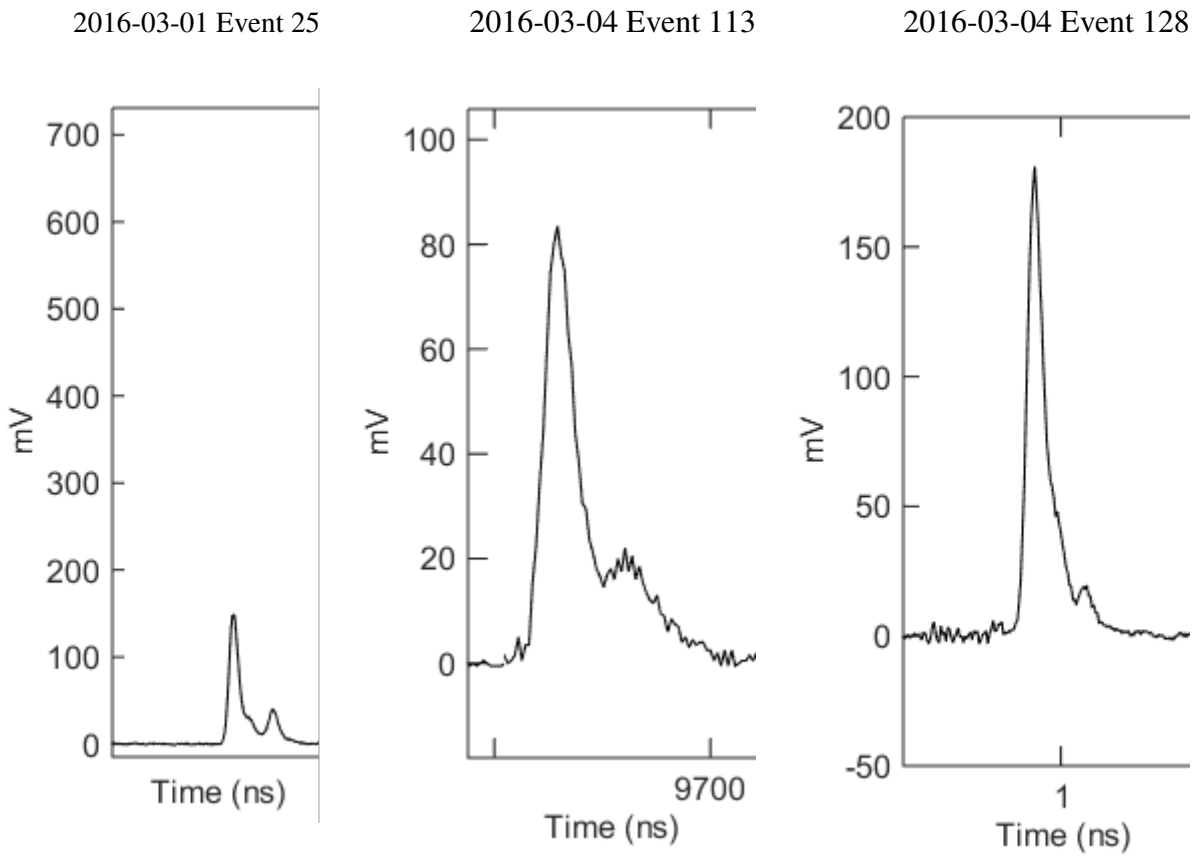

2016-03-04 Event 107

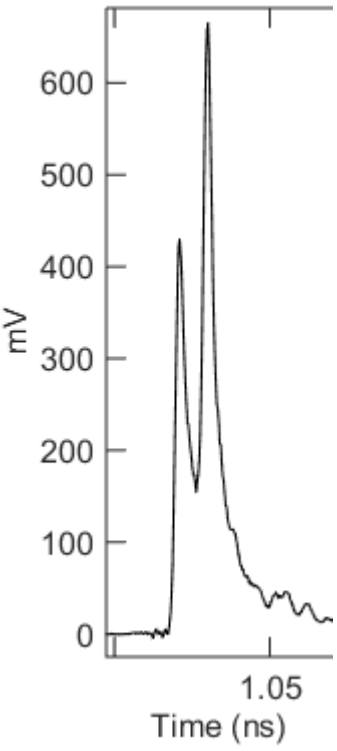

2016-03-10 Event 93

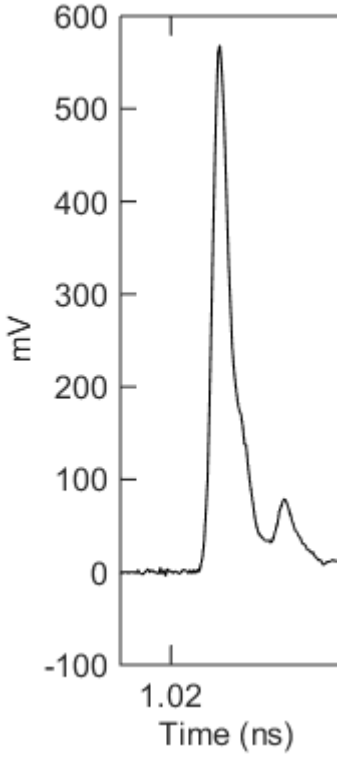

2016-03-10 Event 231

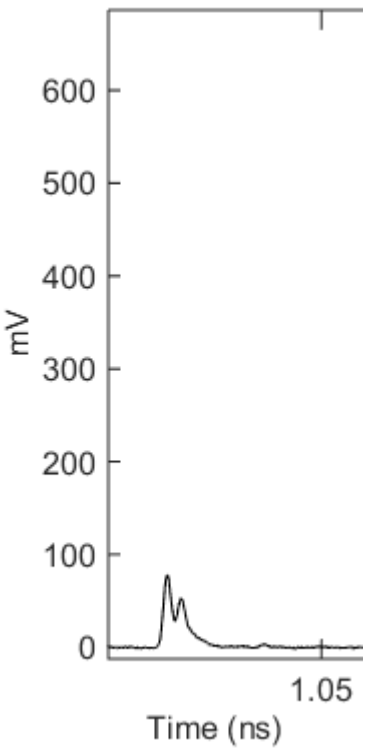

2016-03-10 Event 35

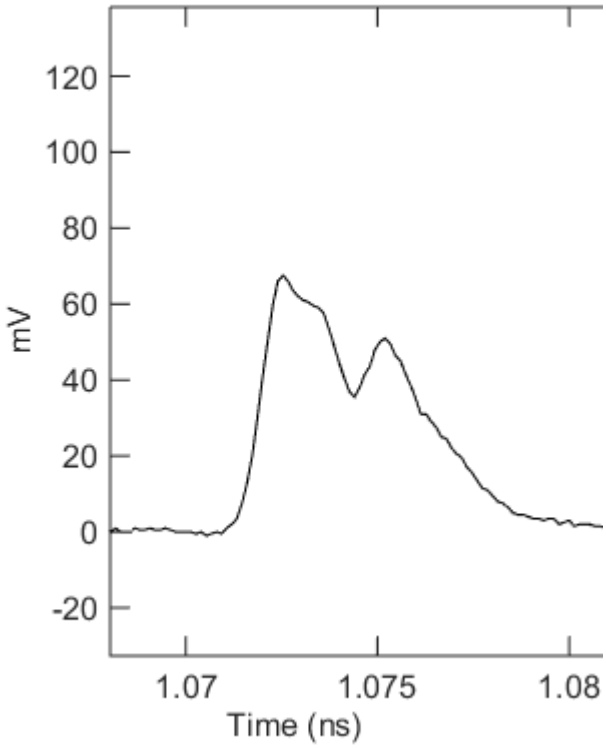

4.2 Conclusions and Future Work

After applying our validity tests and taking into consideration the energy characteristics of neutrons from californium-252 we have a handful of valid double-recoil events. Therefore, we have been successful in detecting double-recoil double-capture events within a single capture-gated detector. We have simply scratched the surface and there is much more to be explored.

As always, more data may be collected which would lead to more double-recoil double-capture events. Having additional, valid events will provide better statistics when comparing characteristics and looking for trends.

Adjustments to the analytical code could also assist in finding double-recoil events. Currently, there is code under development within the group which focuses on the recoils and the sorting of potentially valid events based on the shape of the recoil rather than the presence of double-captures.

We have also considered implementing a technique used by the BYU Nuclear Research group to remove room return. They have mobilized their data acquisition setup and taken it out-of-doors on a scissor lift. By raising their entire setup off of the ground they are able to essentially remove room return.

Another facet to consider is the source itself. Our californium-252 source is composed of californium plated on a wire encased in a stainless steel cylinder. The configuration of this source introduces 97% noise since all decay events are gamma tagged, but only 3% are spontaneous fission events. Within our group, a new source configuration is under investigation which would decrease the noise and allow us to have fission fragment tagged events. This would provide a cleaner source, more verifiable events and less data to process (Ellsworth 2016).

As we continue searching for paired neutrons the next experimental step is to set up a second detector at 30 degrees from the first, relative to the source, and simultaneously acquire data from each detector. Theory suggests that an angular distribution of paired neutrons peaks at zero degree separation between neutrons and levels out at 30 degrees between neutrons. If we are able to

detected paired neutrons by overlaying the signal from these two detectors and they are within the same timing resolution we have established for pairs within a single detector we can prove that the pairs we are detecting are truly pairs (Czirr 2016). Having two detectors will also increase our detection rates of paired neutrons within a single detector, thereby assisting with statistics and trend data.

Appendix A

Double-Recoil Events

This appendix includes plots for the seven double-recoil events detected during March 2016.

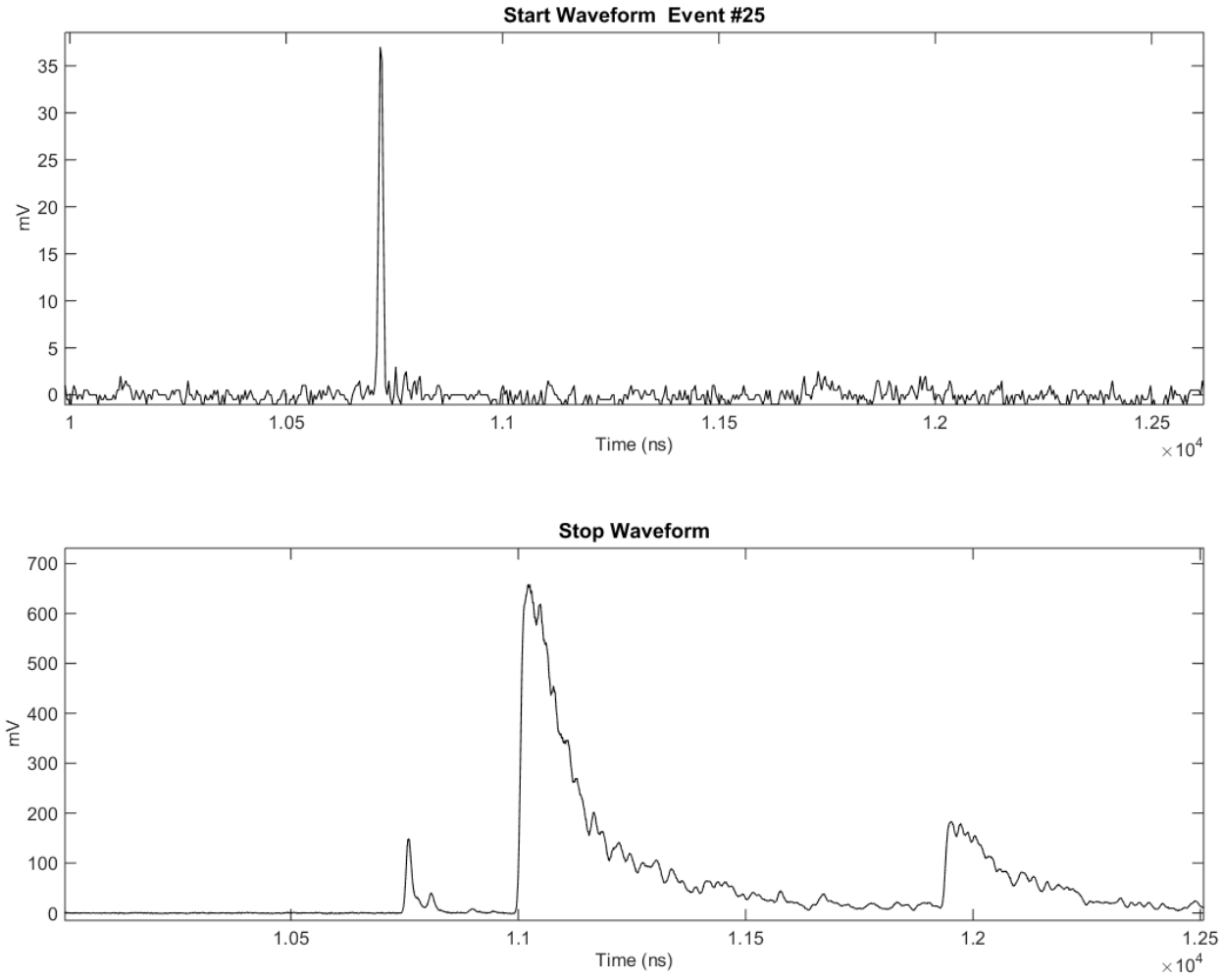

Figure A.1 Double-recoil event number 25 detected on 01 March 2016 using a Hamamatsu PMT.

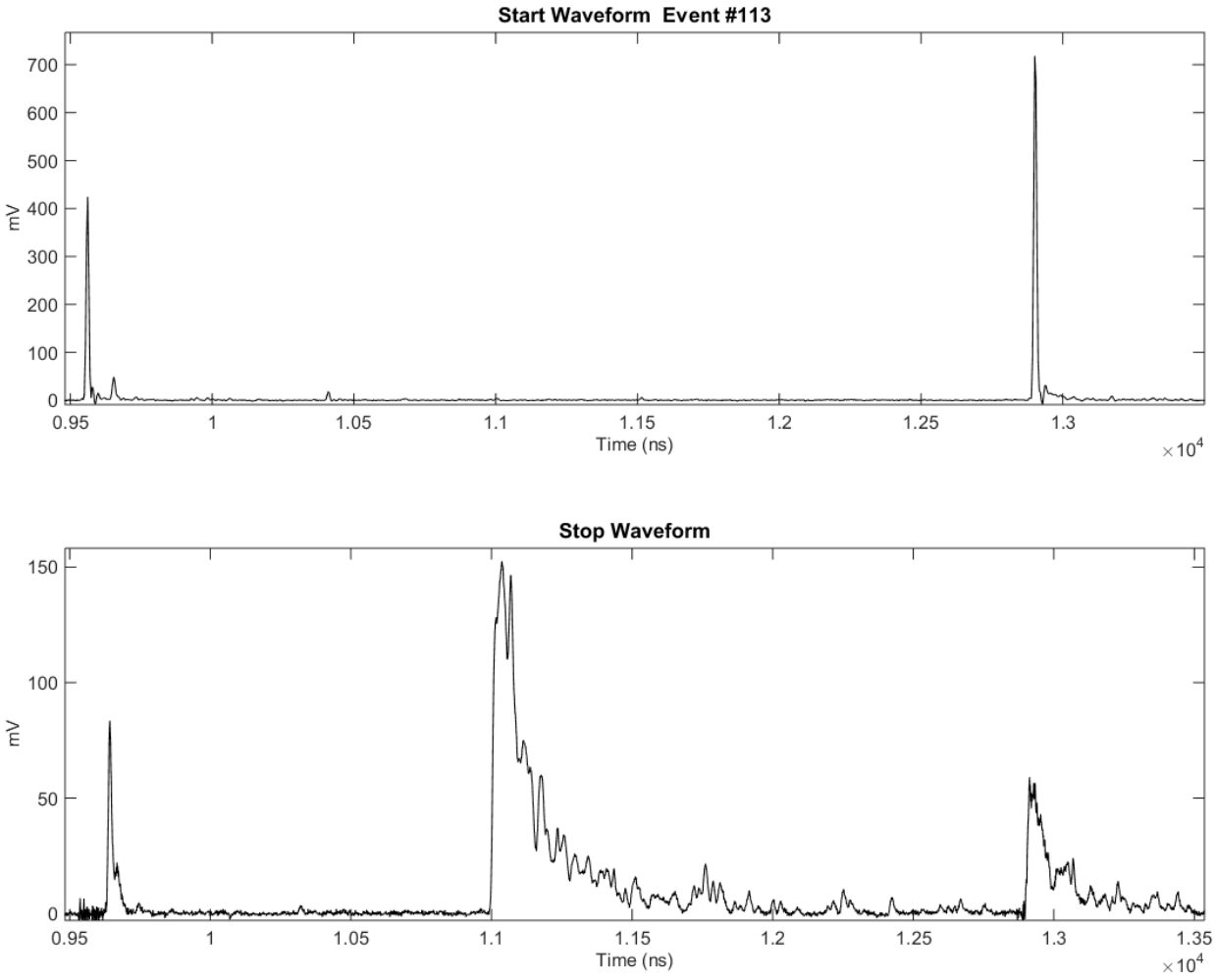

Figure A.2 Double-recoil event number 113 detected on 04 March 2016 using a Hamamatsu PMT.

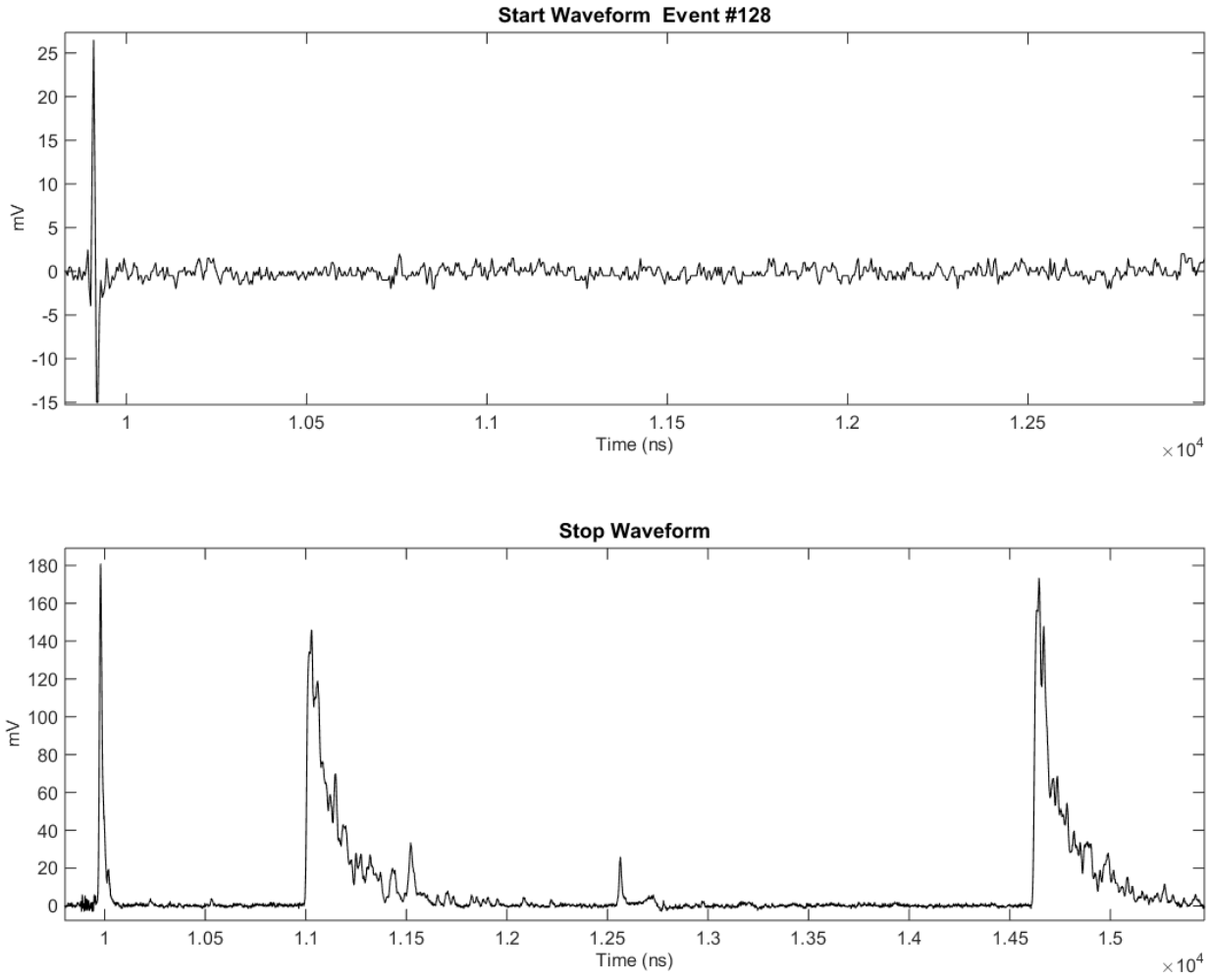

Figure A.3 Double-recoil event number 128 detected on 04 March 2016 using a Hamamatsu PMT.

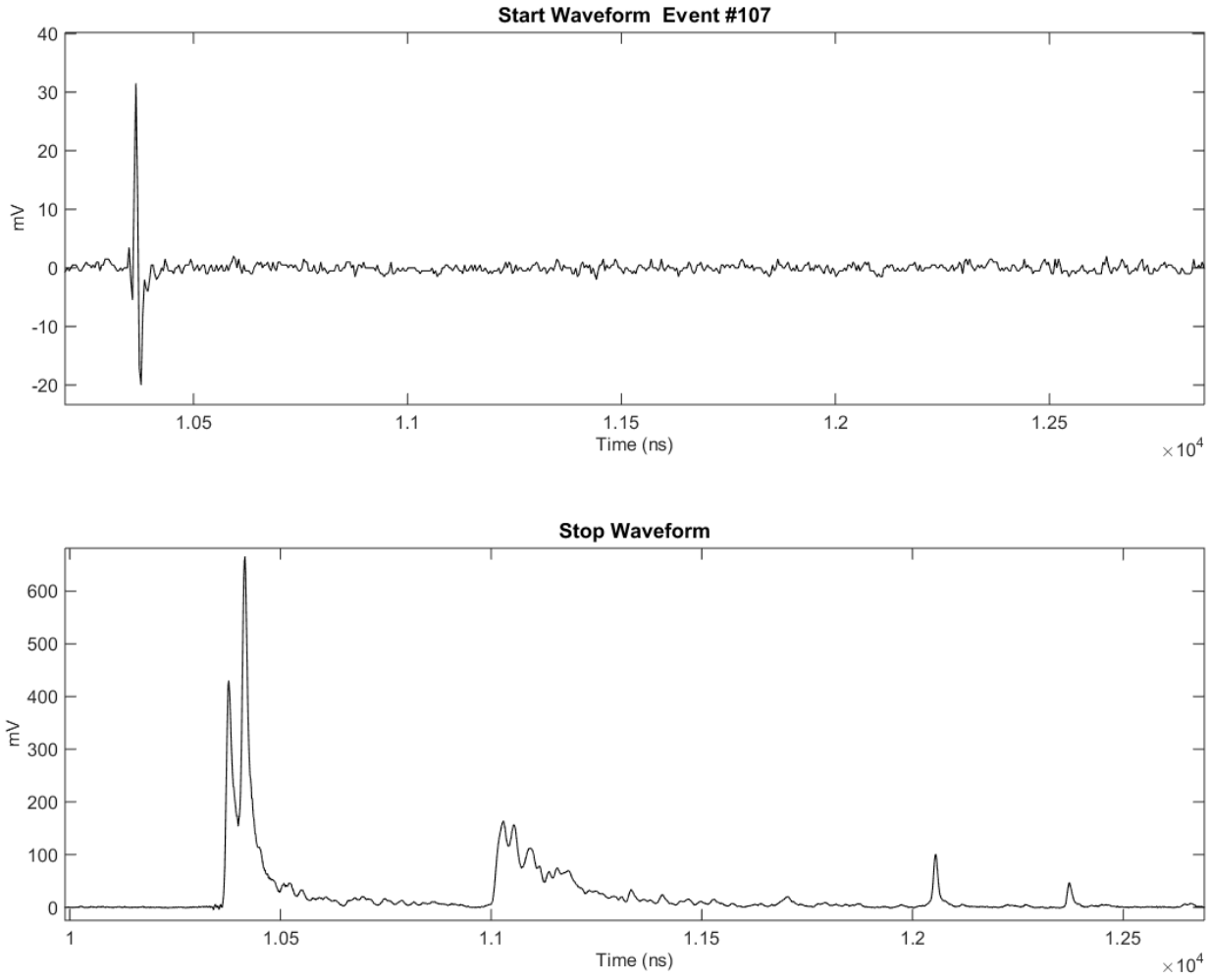

Figure A.4 Double-recoil event number 107 detected on 04 March 2016 using a Hamamatsu PMT.

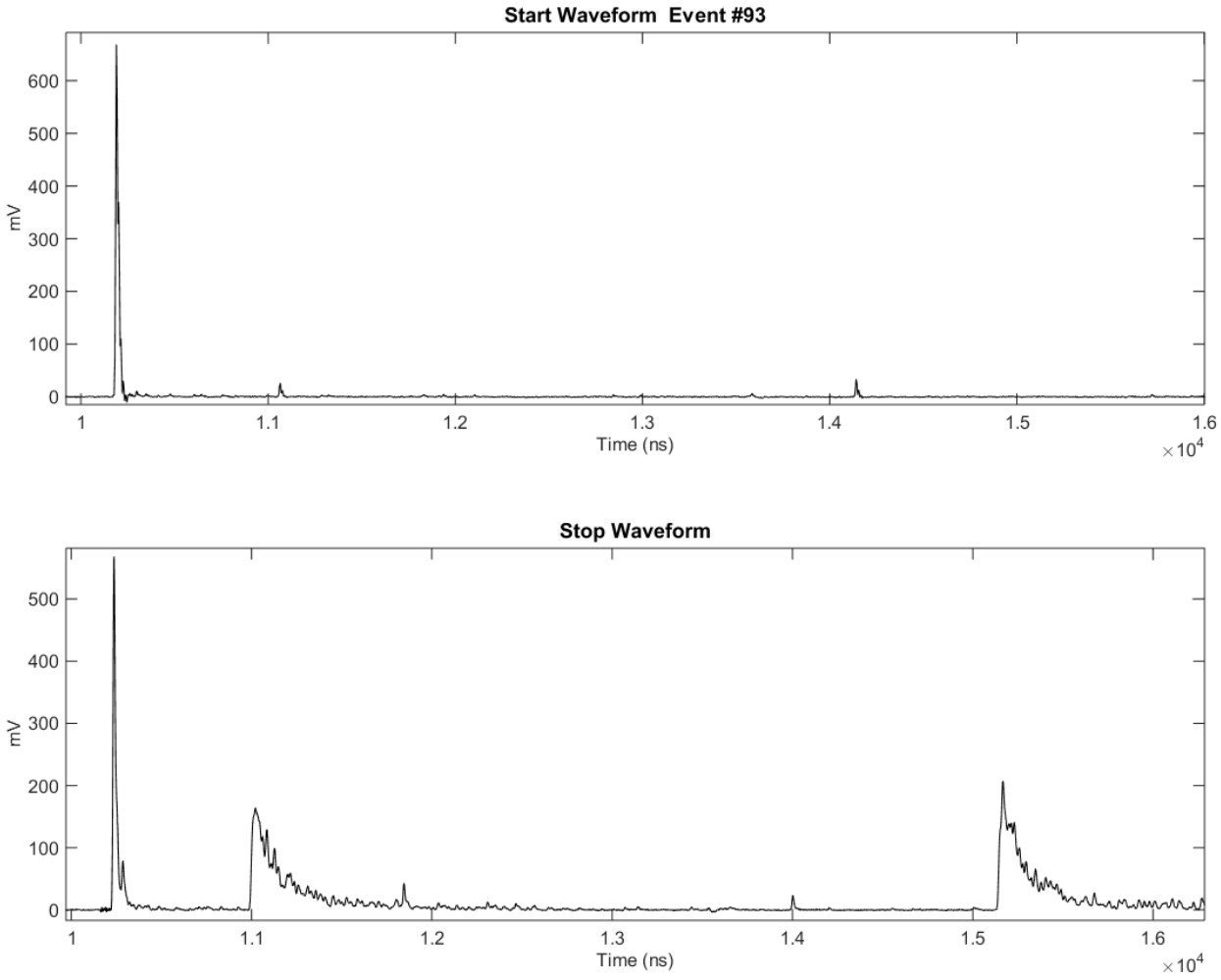

Figure A.5 Double-recoil event number 93 detected on 10 March 2016 using a Hamamatsu PMT.

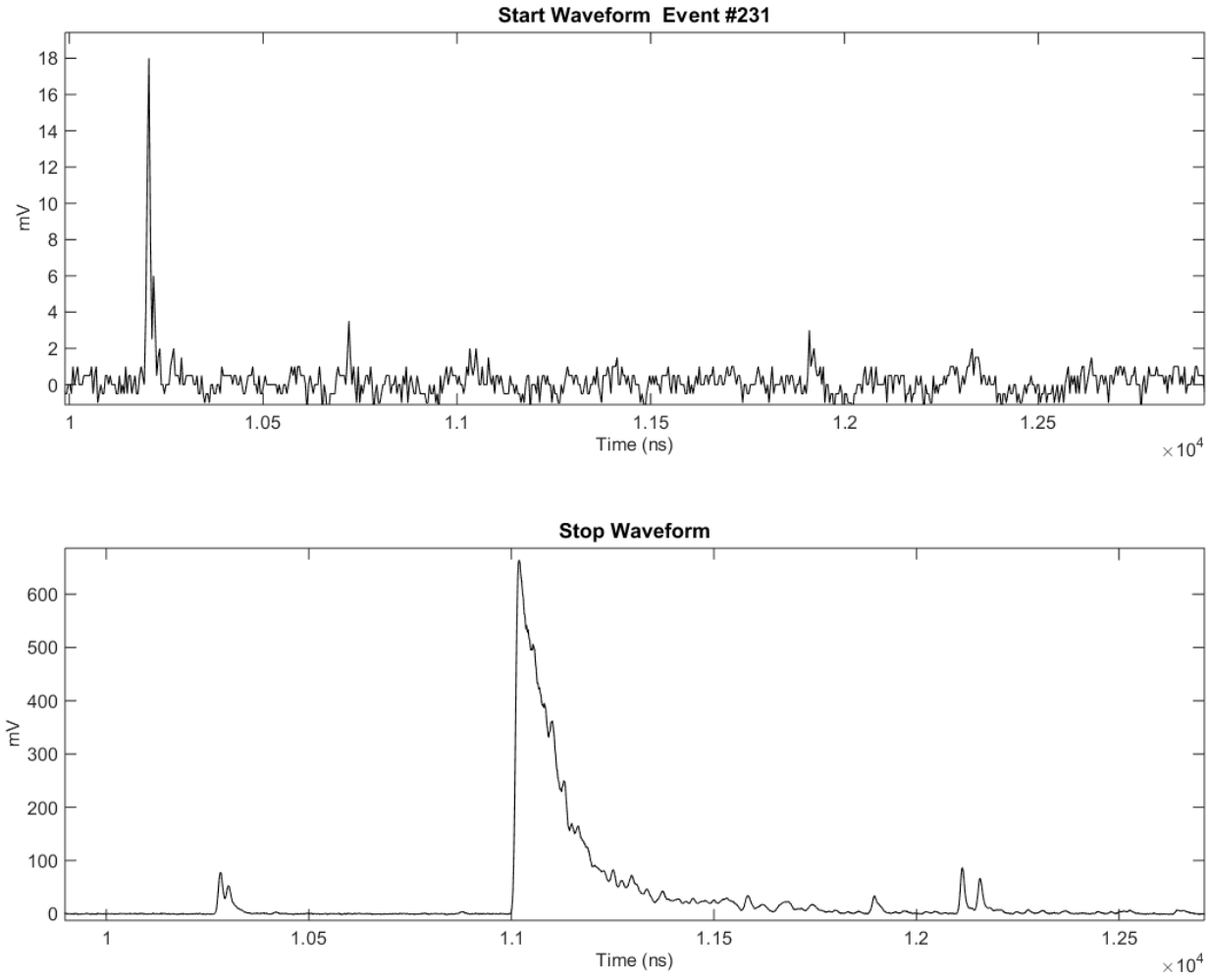

Figure A.6 Double-recoil event number 231 detected on 10 March 2016 using a Hamamatsu PMT.

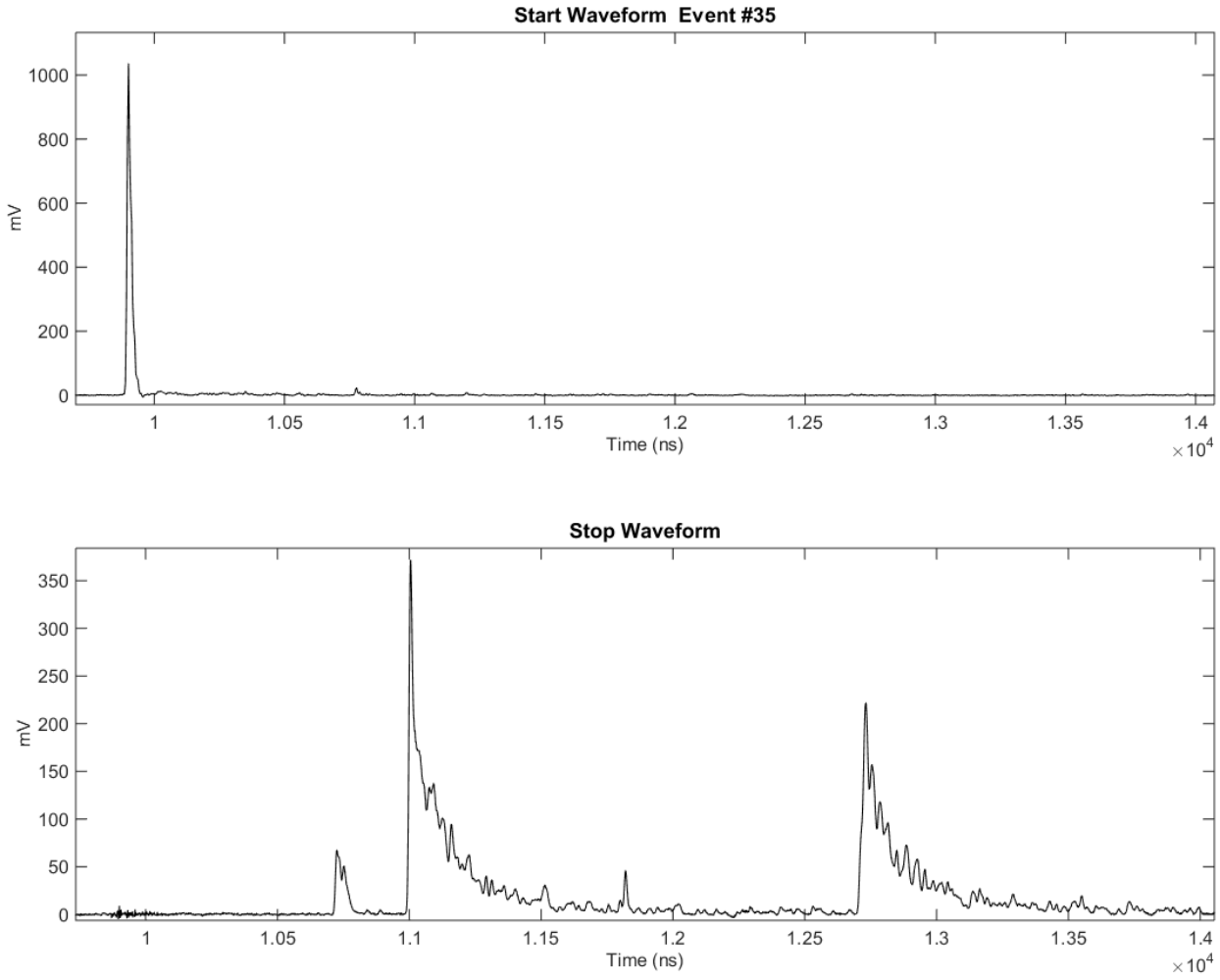

Figure A.7 Double-recoil event number 35 detected on 10 March 2016 using a Hamamatsu PMT.

Appendix B

Californium-252

This appendix includes information on californium-252. Table B.1 contains published characteristics of the activity rates, decay types and neutron energies of californium-252 (Martin et al. 1999). Table B.2 contains previously calculated energies and times of flight for neutrons emitted from spontaneous fission of californium-252 (times and energies are for a distance of one meter between source and detector).

Table B.1 Properties of californium-252.

Alpha Emission	96.91%
Spontaneous Fission	3.09%
Half-Life	2.645 yrs
Neutron Emission	$2.314 \times 10^6 \, /\mathrm{s} \cdot \mu\mathrm{g}$
Most Probable Energy	0.7 MeV
Average Energy	2.1 MeV
Average Neutrons/Fission	3.7

Neutrons emitted from spontaneous fission have a range of energies which can be determined relativistically from the time of flight. The following equations can be used to calculate the energy

$$KE = (\gamma - 1)\, mc^2 \qquad \text{with} \qquad \gamma = \frac{1}{\sqrt{1 - (v^2/c^2)}}.$$

Table B.2 Tabulated energies with respective times of flight for neutrons emitted from californium-252 with a meter between detector and source.

Energy (MeV)	Time of Flight (ns)		Energy (MeV)	Time of Flight (ns)
0.01	723		1.5	59
0.1	229		1.6	51
0.2	162		1.7	55
0.3	132		1.8	54
0.4	114		1.9	52
0.5	102		2.0	51
0.6	93		3.0	42
0.7	86		4.0	36
0.8	81		5.0	32
0.9	76		6.0	30
1.0	72		7.0	27
1.1	69		8.0	26
1.2	66		9.0	24
1.3	63		10.0	23
1.4	61			

Appendix C

Equipment and Setup

Table C.1 Detailed list of equipment used during this project.

Piece of Equipment	Model Number	Serial Number	Additional Information
High Voltage Power Supply	Ortec 556	2408	Rev 29
High Voltage Power Supply	Ortec 556	2133	Rev 28
PMT Base	Ellsworth	11B03	R1250
PMT Base	BYU PHYS ASTRO VAC LAB	11929	–
PMT	Hamamatsu R1250	–	Start Detector
PMT	Hamamatsu	2011-08	Stop Detector
Timing Filter AMP	Ortec 474	11048676	Rev L
Timing Filter AMP	Ortec 474	2145	Rev 21
Desktop Digitizer	CAEN DT5720	0030	–

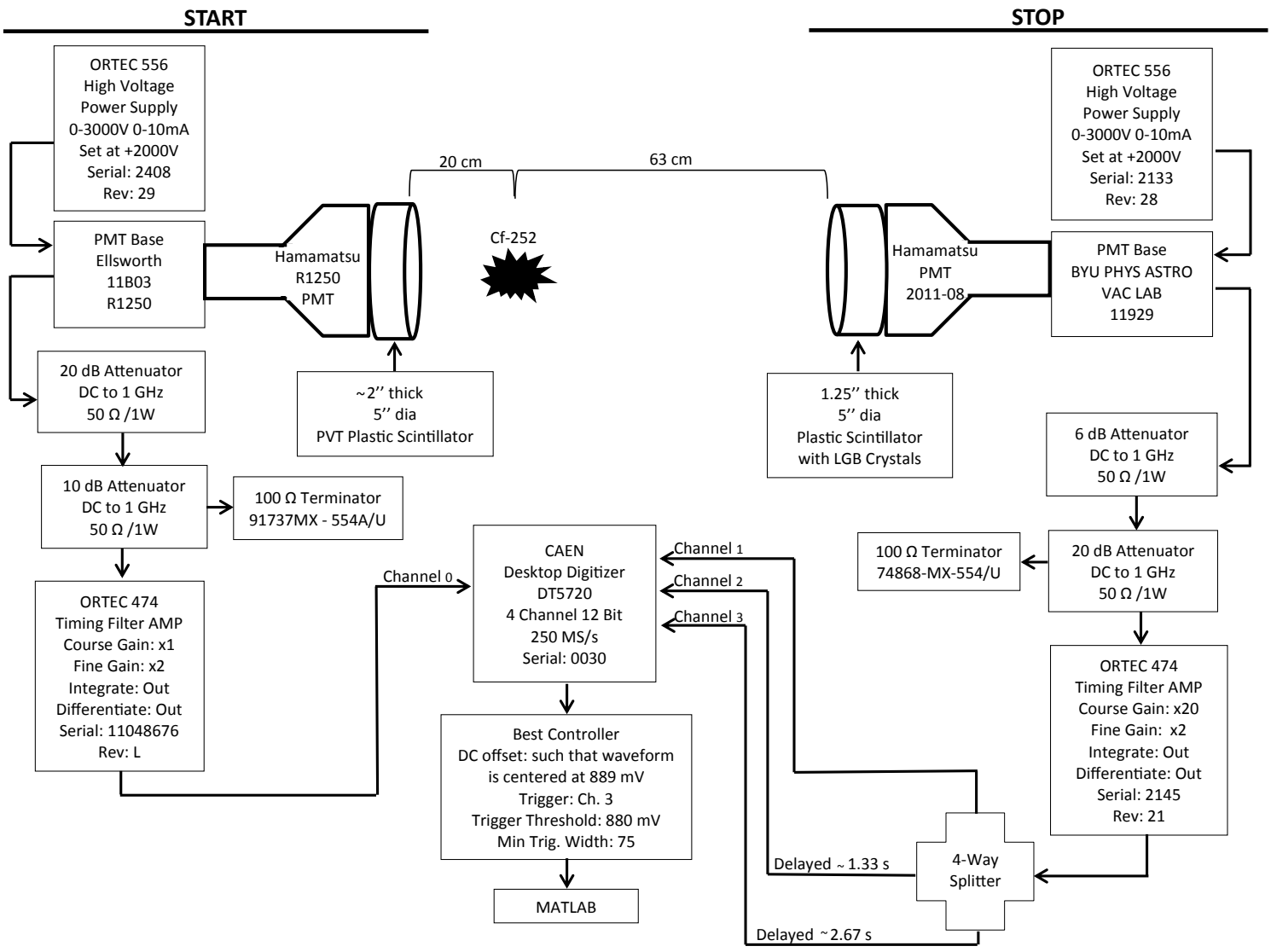
START
STOP
ORTEC 556
High Voltage
Power Supply
0-3000V 0-10mA
Set at +2000V
Serial: 2408
Rev: 29
PMT Base
Ellsworth
11B03
R1250
Hamamatsu
R1250
PMT
20 cm
63 cm
Cf-252
Hamamatsu
PMT
2011-08
PMT Base
BYU PHYS ASTRO
VAC LAB
11929
ORTEC 556
High Voltage
Power Supply
0-3000V 0-10mA
Set at +2000V
Serial: 2133
Rev: 28
20 dB Attenuator
DC to 1 GHz
50 Ω /1W
~2'' thick
5'' dia
PVT Plastic Scintillator
1.25'' thick
5'' dia
Plastic Scintillator
with LGB Crystals
6 dB Attenuator
DC to 1 GHz
50 Ω /1W
10 dB Attenuator
DC to 1 GHz
50 Ω /1W
100 Ω Terminator
91737MX - 554A/U
100 Ω Terminator
74868-MX-554/U
20 dB Attenuator
DC to 1 GHz
50 Ω /1W
CAEN
Desktop Digitizer
DT5720
4 Channel 12 Bit
250 MS/s
Serial: 0030
Channel 0
Channel 1
Channel 2
Channel 3
ORTEC 474
Timing Filter AMP
Course Gain: x1
Fine Gain: x2
Integrate: Out
Differentiate: Out
Serial: 11048676
Rev: L
ORTEC 474
Timing Filter AMP
Course Gain: x20
Fine Gain: x2
Integrate: Out
Differentiate: Out
Serial: 2145
Rev: 21
Best Controller
DC offset: such that waveform
is centered at 889 mV
Trigger: Ch. 3
Trigger Threshold: 880 mV
Min Trig. Width: 75
4-Way
Splitter
Delayed ~ 1.33 s
Delayed ~ 2.67 s
MATLAB

Appendix D

Adit and Hamamatsu PMT Datasheets

This appendix includes data sheets for the Adit B133D01 and Hamamatsu R1250 photomultiplier tubes ((Adit 2004) (Hamamatsu Photonics K.K. 1999)). For more assistance in understanding and comparing photomultiplier tubes see ET Enterprises' pamphlet *Understanding Photomultipliers* (ET Enterprises Limited 2011).

B133D01 Photomultiplier Tube

The B133D01 is a 5" diameter 10-stage end-on photomultiplier with extended sensitivity in the blue, green and red. Designed for scintillation counting and other applications where high quantum efficiency, low dark current, good collection efficiency, and gain stability are of paramount importance.

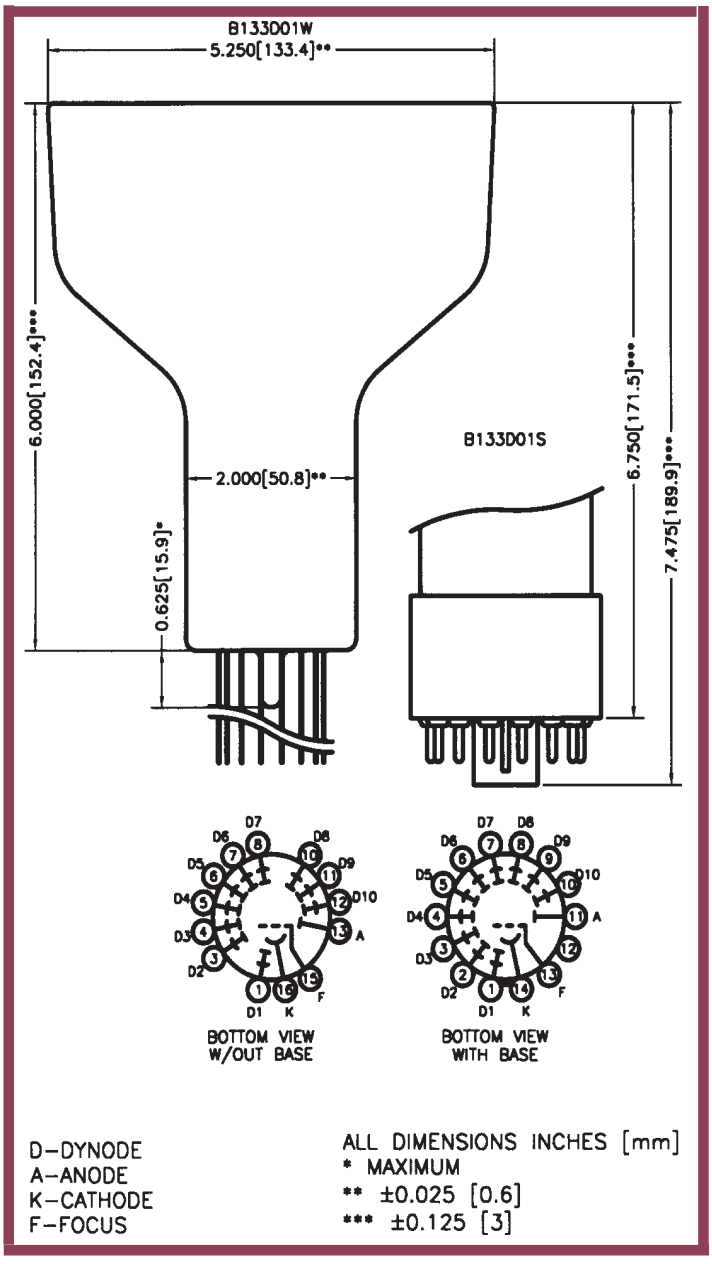

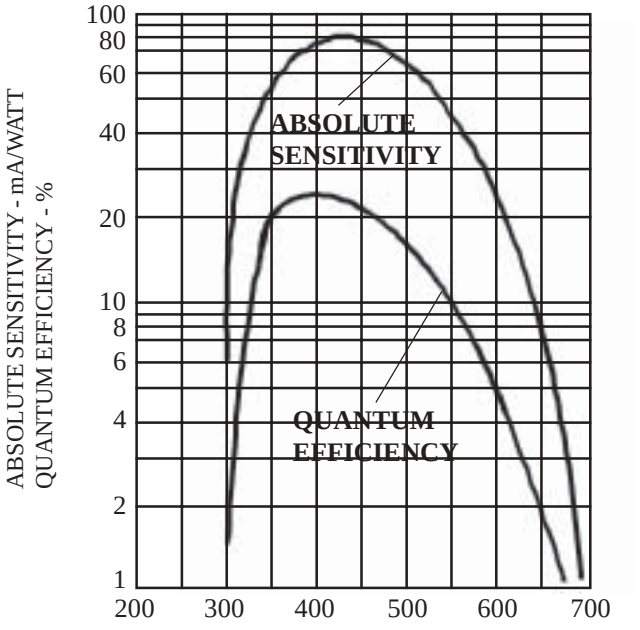

TYPICAL SPECTRAL RESPONSE CHARACTERISTICS

FIGURE 1

Photocathode: Semitransparent Extended Bialkali	
Spectral Response	See Figure 1
Wavelength of maximum response	470 ± 50 nm
Minimum diameter	119.38 mm
Window shape	plano-plano, circular
Window index of refraction @ 436 nm	1.523
Dynodes	BeCu, Box & Grid
Capacitance (anode to all electrodes)	9.5 pF
Operating position	Any
Weight	655 grams

Rev. 01/04

B133D01 Photomultiplier Tube

ELECTRICAL OPERATING RATINGS

	MINIMUM	TYPICAL	MAXIMUM[5]	UNITS
Cathode to dynode No. 1 voltage	40	150	300	VDC
Cathode to anode voltage		1100	1500	VDC
Voltage between consecutive dynodes			100	VDC
Ambient storage temperature		23	60	ºC
Anode current, average over 30 sec.			1.0	µA
Cathode current		1	5	µA
Cathode luminous sensitivity:[1] With 2854° K tungsten source With blue light source[2] With red light source[3]	 80 5 5	 120 12 10	 180 15 15	 µA/lm µA/lm(B) µA/lm(R)
Quantum efficiency @ 420 nm		25		%
Cathode radiant sensitivity @ 420 nm @ 540 nm @ 600 nm @ 680 nm		97 45 25 4		mA/W
Anode luminous sensitivity1100 VDC: With 2854° K tungsten source of 1 x 10^{-3} lm	3	20	50	A/lm
Current amplification @1100 VDC		1 X 10^{6}		
Anode dark current [4] @ 22° C	1	10	20	nA

(1) With 150 VDC between cathode and all other elements connected as anode.

(2) This measurement is made with a blue filter (Corning CS-5-58, 1/2 stock thickness) interposed between a calibrated 2854° K tungsten light source and the photocathode. The (B) appearing in the units signifies that the measurement is made with the blue filter in place.

(3) This measurement is made with a red filter (Corning CS-2-62) interposed between a calibrated 2854° K tungsten light source and the photocathode. The (R) appearing in the units signifies that the measurement is made with the red filter in place.

(4) Measured at the supply voltage which gives an anode sensitivity of 20 A/lm

(5) Recommended operating maximums.

NOTE: When ordering one of the following basing options must be added, i.e. B133D01S

BASING OPTIONS: L - Long Base S - Short Base W - Wire Leads (No Base)

Voltage dividers available made to customer specifications.

ADIT
P.O. Box 870 • 300 Crane • Sweetwater, Texas 79556
800-399-4557 • 915-235-1418 • Fax: 915-235-2872 • E-mail: adit@aditpmt.com • Website: www.aditpmt.com

HAMAMATSU

PHOTOMULTIPLIER TUBE
R1250

For High Energy Physics, Fast Time Response, High Pulse Linearity
127mm (5 Inch) Diameter, Bialkali Photocathode, 14-Stage, Head-on Type

GENERAL

Parameter		Description/Value	Unit
Spectral Response		300 to 650	nm
Wavelength of Maximum Response		420	nm
Photocathode	Material	Bialkali	—
	Minimum Useful Diameter	120	mm dia.
Window	Material	Borosilicate glass	—
Dynode	Structure	Linear focused	—
	Number of Stages	14	—
Base		20-pin base	—
Suitable Socket		E678-20A (supplied)	—

MAXIMUM RATINGS (Absolute Maximum Values)

Parameter		Value	Unit
Supply Voltage	Between Anode and Cathode	3000	Vdc
	Between Anode and Last Dynode	500	Vdc
Average Anode Current		0.2	mA
Ambient Temperature		-30 to +50	°C

CHARACTERISTICS (at 25°C)

Parameter		Min.	Typ.	Max.	Unit
Cathode Sensitivity	Luminous (2856K)	55	70	—	μA/lm
	Blue (with CS 5-58 filter)	7.0	9.0	—	μA/lm-b
	Quantum Efficiency at 390nm	—	22	—	%
Anode Sensitivity	Luminous (2856K)	300	1000	—	A/lm
	Blue (with CS 5-58 filter)	—	130	—	A/lm-b
Gain		—	1.4×10^7	—	—
Anode Dark Current (after 30min. storage in darkness)		—	50	300	nA
Time Response	Anode Pulse Rise Time	—	2.5	—	ns
	Electron Transit Time	—	54	—	ns
	Transit Time Spread	—	1.2	—	ns
Pulse Height Resolution with ^{137}Cs		—	8.3	—	%
Gain Deviation	Long Term	—	1.0	—	%
	Short Term	—	1.0	—	%
Pulse Linearity *	2% Deviation	—	160	—	%
	5% Deviation	—	250	—	%

* Measured with special voltage distribution ratios shown in the Table 2.

Table 1: VOLTAGE DISTRIBUTION RATIO AND SUPPLY VOLTAGE

Electrode	K	G1	G2	Dy1	Dy2	Dy3	Dy4	Dy5	Dy6	Dy7	Dy8	Dy9	Dy10	Dy11	Dy12	Dy13	Dy14	P
Ratio	2.5	7.5	0	1.2	1.8	1	1	1	1	1	1	1	1	1.5	1.5	3	2.5	

Supply Voltage: 2000Vdc, K: Cathode, Dy: Dynode, P: Anode, G: Grid

Table 2: SPECIAL VOLTAGE DISTRIBUTION RATIO AND SUPPLY VOLTAGE FOR PULSE LINEARITY MEASUREMENT

Electrode	K	G1	G2	Dy1	Dy2	Dy3	Dy4	Dy5	Dy6	Dy7	Dy8	Dy9	Dy10	Dy11	Dy12	Dy13	Dy14	P
Ratio	2.5	7.5	0	1.2	1.8	1	1	1	1	1.2	1.5	2	2.8	4	5.7	8	5	
Capacitors in μF											0.01	0.01	0.02	0.02	0.02	0.04	0.06	

Supply Voltage: 2500Vdc, K: Cathode, Dy: Dynode, P: Anode, G: Grid

PHOTOMULTIPLIER TUBE R1250

Figure 1: Typical Spectral Response

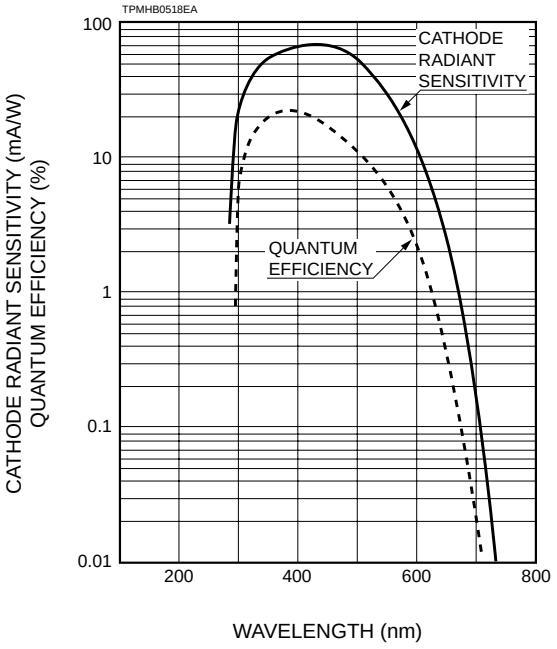

Figure 2: Typical Gain Characteristics

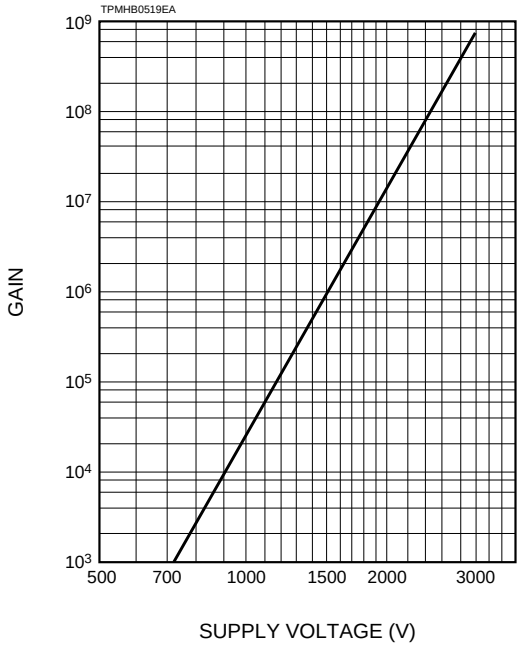

Figure 3: Dimensional Outline and Basing Diagram (Unit: mm)

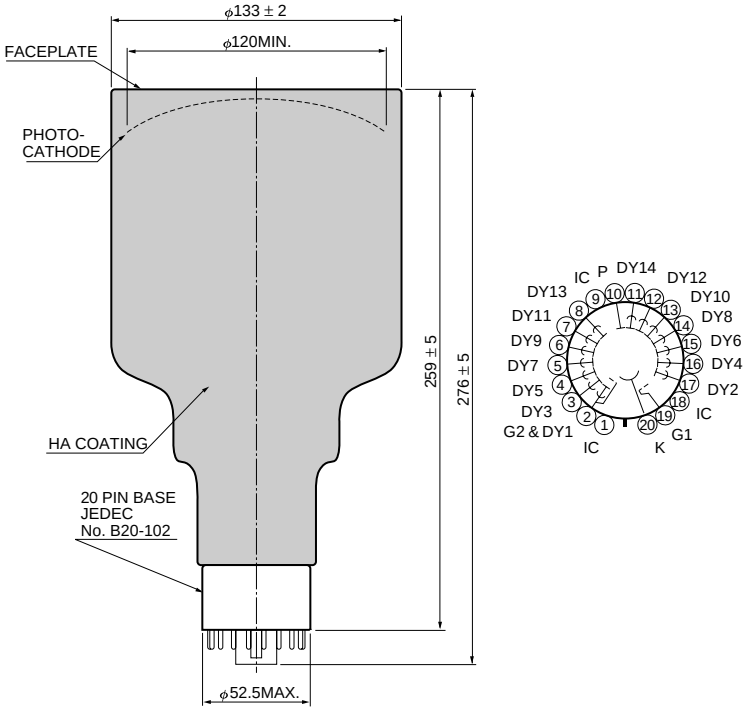

Socket (E678-20A)

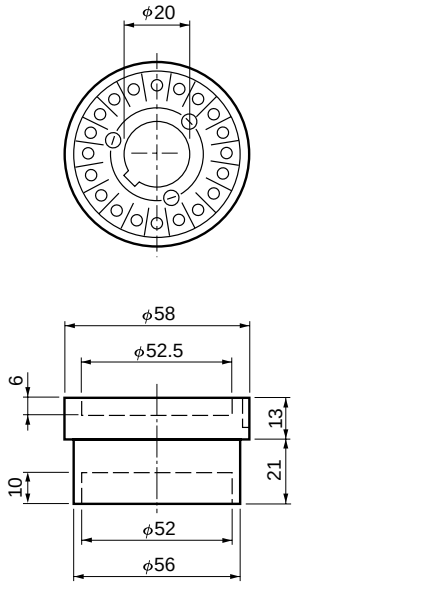

HAMAMATSU HOMEPAGE URL http://www.hamamatsu.com

HAMAMATSU PHOTONICS K.K., Electron Tube Center
314-5, Shimokanzo, Toyooka-village, Iwata-gun, Shizuoka-ken, 438-0193, Japan, Telephone: (81)539/62-5248, Fax: (81)539/62-2205

U.S.A.: Hamamatsu Corporation: 360 Foothill Road, P. O. Box 6910, Bridgewater. N.J. 08807-0910, U.S.A., Telephone: (1)908-231-0960, Fax: (1)908-231-1218
Germany: Hamamatsu Photonics Deutschland GmbH: Arzbergerstr. 10, D-82211 Herrsching am Ammersee, Germany, Telephone: (49)8152-375-0, Fax: (49)8152-2658
France: Hamamatsu Photonics France S.A.R.L.: 8, Rue du Saule Trapu, Parc du Moulin de Massy, 91882 Massy Cedex, France, Telephone: (33)1 69 53 71 00, Fax: (33)1 69 53 71 10
United Kingdom: Hamamatsu Photonics UK Limited: Lough Point, 2 Gladbeck Way, Windmill Hill, Enfield, Middlesex EN2 7JA, United Kingdom, Telephone: 44(20)8-367-3560, Fax: 44(20)8-367-6384
North Europe: Hamamatsu Photonics Norden AB: Smidesvägen 12, SE-171-41 SOLNA, Sweden, Telephone: (46)8-509-031-00, Fax: (46)8-509-031-01
Italy: Hamamatsu Photonics Italia: S.R.L.: Strada della Moia, 1/E, 20020 Arese, (Milano), Italy, Telephone: (39)02-935 81 733, Fax: (39)02-935 81 741

TPMH1213E02
DEC. 1999

Appendix E

Analytical Code

This appendix includes the analytical code used to process data taken from Hamamatsu photomultiplier tubes. The first script is the main analysis tool used to process all data. It is a Matlab function called by a previously designed menued mainframe. The second script was used in plotting events which passed the analytical code.

```
%%%%%%%%%%%%%%%%%%%%%%%%%%%%%%%%%%%%%%%%%%%%%%%%%%%%%%%%%%%%%%%%%%%%%%%%%%%%
% ToF Analysis Double Capture Hamamatsu 4 Ch is for stop waveform
% analysis to detect and sort out double capture events from a Hamamatsu
% PMT and 3 channels in the CAEN with time delay (0, 1.3, 2.67).
% This code assumes the following:
%       Gain on start and stop detectors set to 2V Peak-to-Peak
%       Use of headers and structure of CAEN DT5720
%       Use of best controller

% LNAR Group 2015
% John Ellsworth - Group Advisor jee@physics.byu.edu
% Alec Raymond - First Editor alec.raymond@yahoo.com
% KaeCee Terry - Double Capture Editor kaecee.terry@gmail.com
% Double Capture Code adapted from: http://www.mathworks.com/matlabcentral/
%    answers/37363-help-with-identifiny-change-in-curve-shape-automatically
%%%%%%%%%%%%%%%%%%%%%%%%%%%%%%%%%%%%%%%%%%%%%%%%%%%%%%%%%%%%%%%%%%%%%%%%%%%%

function ToFAnalysisDoubleCaptureHamamatsu4Ch(dir,file)

close all
close all hidden % close leftover waitbars

global fields

for i=1:length(fields)
    str1=[fields(i).name,'=',fields(i).val,';'];
    eval(str1); % evaluate string to make and assign 'fields' variables
end

% Constants specific to the CAEN and Best Controller
triggerLocation =round(eventsamples*.6689453125)*3;
% from CAEN digitizer .7*(# samples/event) (but not really...)
timeResolution = 4/3;
% 4ns/sample from CAEN with 3 channel time delay there is 4/3ns resolution

% Initializing vectors
doubleCaptureDataOutput = [];
megaStop=zeros(4096*3,1);
numOfCaptures=0;

for fileNumber = 1:length(file)

    filename=[dir,'/',char(file(fileNumber))];
    fid = fopen(filename);

    nevent=0;

    % preallocate vector
    numEvents = getnum(dir,char(file(fileNumber)));
    ToFV = zeros(1,numEvents);
    timeConstant=zeros(1,numEvents);
    peakWidth=zeros(1,numEvents);
```

```
maxAmpOfPeakIndex=zeros(1,numEvents);
earlyAreaSmoothed=zeros(1,numEvents);
lateAreaSmoothed=zeros(1,numEvents);
totalAreaSmoothed=zeros(1,numEvents);
earlyOverTotalSmoothed=zeros(1,numEvents);
startToPeak=zeros(1,numEvents);
timeConstantCutOff=zeros(1,numEvents);

% clear double capture data
doubleCaptureData=[];

% Progress Bar Initializing
eventCounter=0;
h=waitbar(0,'Please Wait...');

while 1
    % load wfms
    [start,stopDelay0,stopDelay1, stopDelay2]=getdata(fid,eventsamples);

    % check to see if no data was found
    if isempty(start) == 1
        break
    end

    % Progress bar
    eventCounter=eventCounter+1;
    waitbar(eventCounter/numEvents,h, sprintf(...
        'Please Wait...File %d of %d',fileNumber, length(file)));

    % Start Pulse Prep
    start = -start; % invert wfm
    start = start-mode(start); % remove DC offset
    if max(abs(start)) <= noiseLevel
        continue % skip wfm with no signal
    end

    % interpolate start wfm so it has the same length as megaStop
    x = 1:length(start); % samples points
    v = start; % sample values
    xq = 1:1/3:length(start); %query points
    start = interp1(x,v,xq);

    % fill in end of interpolated waveform
    start(end + 1) = start(end - 2);
    start(end + 1) = start(end - 2);

   % Invert wfms
    stopDelay0 = -stopDelay0;
    stopDelay1 = -stopDelay1;
    stopDelay2 = -stopDelay2;

    % Stop Pulse Preparation
    % Find the baseline and offset to 0
```

```
        stopDelay0=stopDelay0-mode(stopDelay0); % remove DC offset
        stopDelay1=stopDelay1-mode(stopDelay1); % remove DC offset
        stopDelay2=stopDelay2-mode(stopDelay2); % remove DC offset
        if max(abs(stopDelay0)) <= noiseLevel
            continue
        end

        % to correctly construct the megaStop add the channels 3-2-1
        indexStep = 1;
        for index = 1:3:length(megaStop)-2
            megaStop(index + 2) = stopDelay0(indexStep);
            megaStop(index + 1) = stopDelay1(indexStep);
            megaStop(index) = stopDelay2(indexStep);
            indexStep=indexStep+1;
        end
        stop = megaStop;

        % For 2V Peak-to-Peak muon strikes are cut off at ~3892 (band-aid)
        if max(abs(stop)) > 3892 % muon threshold
            continue
        end

%         %DEBUG PLOTS - create a waveforms array to hold as many wfms
%         %as you want. Then use the function debugPlots to create
%         %subplots. debugPlots(# subplots desired, waveforms, save?)
%         %For the save option use 1 to save out the plots and 0 to not
%             waveforms(:,1) = start;
%             waveforms(:,2) = stop;
%             debugPlots(size(waveforms,2),waveforms,0)
%             pause
%             clear waveforms
%         % END DEBUG PLOTS

        numOfCaptures = numOfCaptures + 1;
%%%%%%%%%%%%%%%%%%%%%%%%%%%%%%%%%%%%%%%%%%%%%%%%%%%%%%%%%%%%%%%%%%%%%%%%%%%%%%%
        % Finding Double Captures
        % Smooth the stop waveform
        x=1:length(stop);
        dx=1;
        smoothingConst=1e-5;
        % amount of smoothing, the closer to 1 the more details given
        stopSmoothed=csaps(x,stop,smoothingConst);
        % csaps = cubic smoothing spline
        stopPolynomial=ppval(stopSmoothed,x);
        % ppval=evalute piecwise polynomial

        % Find the First Derivative of smoothed stop waveform
        stopFirstDer = nan(size(stopPolynomial));%initialize 1st derivative
        stopFirstDer(2:end-1)=(stopPolynomial(3:end)...
            - stopPolynomial(1:end-2))/(2*dx); % fill in der

        % Find peaks of the absolute value of the 1st Derivative above 1.5
        %   after going through lots of waveforms (for 2V P-to-P) I found
```

```
        %   that 1.5 is a good threshold to start looking for peaks
        [~,slopePeakIndex] = findpeaks(abs(stopFirstDer),...
            'MINPEAKHEIGHT',1.5,'SORTSTR','descend'); % find peaks, sort

        % Select first six peaks (peaks ordered from greatest to least) to
        %   be used in analysis - six is chosen because we are looking for
        %   a change in slope from positive to negative for three peaks on
        %   the original waveform
        if length(slopePeakIndex)<6
            slopePeakIndex = slopePeakIndex(1:length(slopePeakIndex));
        else
            slopePeakIndex = slopePeakIndex(1:6);
            % replace all index values with just first six
        end

        % Count the number of positive peaks - if there are less than 2
        %   peaks continue to the next wfm
        numOfPeaks=sum(stopFirstDer(slopePeakIndex(:))>=1);
        if numOfPeaks <= 2
            continue
        end

        % put indices in ascending order for next part of proceedure
        slopePeakIndex = sort(slopePeakIndex,'ascend');

        % make sure not to drag anything from the last waveform
        clear timeConstant timeConstantCutOff peakWidth maxAmpOfPeakIndex
        clear earlyAreaSmoothed lateAreaSmoothed totalAreaSmoothed
        clear earlyOverTotalSmoothed startToPeak risingEdge fallingEdge ToFV

        % Find properties of peaks on smoothed stop wfm
        for k=1:length(slopePeakIndex)
            % find the peak between two consecutive indices
            clear peakValue peakIndex
            if k==1
                [peakValue,peakIndex]=(findpeaks(...
                    stopPolynomial(1:slopePeakIndex(k))));
            else
                [peakValue,peakIndex]=(findpeaks(...
                    stopPolynomial(slopePeakIndex(k-1):slopePeakIndex(k))));
                peakIndex=peakIndex+slopePeakIndex(k-1)-1;
                % adjust index to correct location
            end

            % if no peak is found, continue to next peak
            if isempty(peakValue)==1 || isempty(peakIndex)==1
                continue
            end

            % if the max peakValue is below the noiseLevel,
            % continue to next peak
            if max(peakValue)<=noiseLevel
                continue
```

```
end

% take the max of the peakValues - the tail of the capture will
% give many peaks, but we only want one peak between each
% set of indices
indexOfMax = find(max(peakValue));
peakValue=peakValue(indexOfMax);
peakIndex=peakIndex(indexOfMax);

% find where the pulse starts
if k<=2
    startOfRisingEdge=find(abs...
        (stopPolynomial(1:peakIndex)) <= noiseLevel,1,'last');
else
    startOfRisingEdge=find(abs...
        (stopPolynomial(slopePeakIndex(k-2):peakIndex))...
        <= noiseLevel,1,'last');
    startOfRisingEdge=startOfRisingEdge+slopePeakIndex(k-2)-1;
    % correct index
end

% if the rising edge cannot be found
%   i.e. when two peaks are on top of each other
if isempty(startOfRisingEdge)==1
    if k-1==0
        startOfRisingEdge=1;
    else
        [~,startOfRisingEdge]=min...
            (stopPolynomial(slopePeakIndex(k-1):peakIndex));
        startOfRisingEdge=...
            startOfRisingEdge+slopePeakIndex(k-1)-1;
        % correct index
    end
end

% Find the rising time of the peak
startToPeak(k)=peakIndex-startOfRisingEdge;

% find where the pulse ends
if k>=2
    endOfFallingEdge=find(abs(stopPolynomial(peakIndex:end))...
        <= noiseLevel,1,'first');
else
    endOfFallingEdge=find(abs...
        (stopPolynomial(peakIndex:slopePeakIndex(k+1)))...
        <= noiseLevel,1,'first');
end

% if the end of the pulse cannot be found (i.e. when two peaks
% are on top of each other) find the minimum value between them
if isempty(endOfFallingEdge)==1
    [~,endOfFallingEdge]=min(stopPolynomial(peakIndex:end));
end
```

```
endOfFallingEdge=endOfFallingEdge+peakIndex-1; % correct index

% if tail never goes below noiseLevel before the end of wfm,
% set end as endOfFallingEdge
if isempty(endOfFallingEdge)==1
    endOfFallingEdge=length(stopPolynomial);
end

% Find double the rise time to use as early cut off point
earlyCutOff=startOfRisingEdge+2.*(peakIndex-startOfRisingEdge);

% If the early cut off point is greater than the end of the
%    falling edge continue to the next event
if earlyCutOff>endOfFallingEdge
    startToPeak(k)=[];
    continue
end

% Find Early, Late & Total Area of pulses on smoothed stop wfm
earlyAreaSmoothed(k)=...
    sum(stopPolynomial(startOfRisingEdge:earlyCutOff));
lateAreaSmoothed(k)=...
    sum(stopPolynomial(earlyCutOff:endOfFallingEdge));
totalAreaSmoothed(k)=...
    sum(stopPolynomial(startOfRisingEdge:endOfFallingEdge));

% Calculate the Early/Total Fraction
earlyOverTotalSmoothed(k)=...
    earlyAreaSmoothed(k)/totalAreaSmoothed(k);

% if there is a recoil in the tail - skip that peak
if  peakIndex > triggerLocation &&...
        earlyOverTotalSmoothed(k) > 0.8
    earlyOverTotalSmoothed(k) =[];
    startToPeak(k)=[];
    totalAreaSmoothed(k)=[];
    lateAreaSmoothed(k)=[];
    earlyAreaSmoothed(k)=[];
    continue
end

% calculate the width of the pulse
peakWidth(k)=endOfFallingEdge-startOfRisingEdge;

% calculate 1/e*peak which gives 36.8% of the peak
timeConstantCutOff(k)=peakValue*(1/exp(1));

% find where on the pulse is the value 36.8% of the peak
[~,timeConstantPoint]=...
min(abs(stopPolynomial(peakIndex:endOfFallingEdge)...
- timeConstantCutOff(k)));
timeConstantPoint=peakIndex+timeConstantPoint-1;
%keep index counting from beginning
```

```
% calculate the time constant
timeConstant(k)=timeConstantPoint-peakIndex;

% save out index of max amplitude of peak (used in plotting)
maxAmpOfPeakIndex(k)= peakIndex;

% Find the "start" of the pulse -- 1/3 up the rising edge
if earlyOverTotalSmoothed(k)>0.8 % if the peak is a recoil
    if peakIndex - recoilPeakCFDWindow < 1
        [~,startIndexOfPeak]=...
        min(abs(stopPolynomial(1:peakIndex)...
        - constFracDisc*peakValue));
    else
        [~,startIndexOfPeak]=...
        min(abs(stopPolynomial(peakIndex-recoilPeakCFDWindow:...
            peakIndex) - constFracDisc*peakValue));
        startIndexOfPeak=...
            peakIndex-recoilPeakCFDWindow+startIndexOfPeak-1;
        %keep index counting from beginning
    end
else % if the peak is not a recoil
    if peakIndex - stopPeakCFDWindow < 1
        [~,startIndexOfPeak]=...
        min(abs(stopPolynomial(1:peakIndex)...
        - constFracDisc*peakValue));
    else
        [~,startIndexOfPeak]=...
        min(abs(stopPolynomial(peakIndex-stopPeakCFDWindow:...
            peakIndex) - constFracDisc*peakValue));
        startIndexOfPeak=...
            peakIndex-stopPeakCFDWindow+startIndexOfPeak-1;
        %keep index counting from beginning
    end
end

% "Time of Flight" Vector
if earlyOverTotalSmoothed(k)>0.8 % if the peak is a recoil
    if max(start(1:startIndexOfPeak))<=noiseLevel
        continue
    end

    % Find all of the start peak is above the noiseLevel
    [~,startIndex] =...
        findpeaks(start(1:startIndexOfPeak),'MINPEAKHEIGHT',15);
    if isempty(startIndex)==1
        continue
    end

    for s=length(startIndex):-1:1

        % Start with peak closest to recoil (and work backwards)
        closestStartIndex = startIndex(s);
```

```
            % Find rising edge of start
            startRisingEdge = [];
            startFallingEdge = [];

            if closestStartIndex-stopPeakCFDWindow < 1
                startRisingEdge =...
                    find(abs(start(1:closestStartIndex))...
                    <= noiseLevel,1,'last');
            else
                startRisingEdge = ...
                    find(abs(start(closestStartIndex-...
                    stopPeakCFDWindow:closestStartIndex))...
                    <= noiseLevel,1,'last');
                startRisingEdge = ...
                    startRisingEdge+closestStartIndex...
                        -stopPeakCFDWindow-1;
            end

            if isempty(startRisingEdge)==1
                continue
            end

            % Find falling edge of start
            startFallingEdge =...
                find(abs(start(closestStartIndex:end))...
                <= noiseLevel,1,'first');
            startFallingEdge = startFallingEdge+closestStartIndex-1;

            if isempty(startFallingEdge)==1
                continue
            end

            if startFallingEdge-startRisingEdge <10
                continue
            else
                break
            end
        end

        if isempty(startRisingEdge)==1
            continue
        else
            % Find start peak value
            [startValue,startValueIndex] =...
                max(start(startRisingEdge:startFallingEdge));
            startValueIndex = startValueIndex+startRisingEdge-1;

            % Start Pulse CFD
            [~,startIndexOfStartWfm] =...
                min(abs(start(startRisingEdge:startValueIndex)...
                - constFracDisc*startValue));
            startIndexOfStartWfm=...
```

```
                    startIndexOfStartWfm+startRisingEdge-1;

            end

                if isempty(startIndexOfStartWfm)==1
                    continue
                end

            ToFV(k)=...
                (startIndexOfPeak-startIndexOfStartWfm)/timeResolution;
            % if the time of flight is negative - skip that peak
            if ToFV(k) <=0
                timeConstant(k)=[];
                peakWidth(k)=[];
                maxAmpOfPeakIndex(k)=[];
                earlyAreaSmoothed(k)=[];
                lateAreaSmoothed(k)=[];
                totalAreaSmoothed(k)=[];
                earlyOverTotalSmoothed(k)=[];
                startToPeak(k)=[];
                ToFV(k)=[];
                continue
            end
        else
            ToFV(k)=0;
        end
    end

    % Check to make sure timeConstant exists (for muon strikes (?) all
    % the rise times are less than 15 so timeConstant is not created)
    if exist('timeConstant')==0
        continue
    end
    if isempty(timeConstant)==1
         continue
    end

    % Find zeros and then delete them
    timeConstant(timeConstant==0)=[];
    peakWidth(peakWidth==0)=[];
    maxAmpOfPeakIndex(maxAmpOfPeakIndex==0)=[];
    earlyAreaSmoothed(earlyAreaSmoothed==0)=[];
    lateAreaSmoothed(lateAreaSmoothed==0)=[];
    totalAreaSmoothed(totalAreaSmoothed==0)=[];
    earlyOverTotalSmoothed(earlyOverTotalSmoothed==0)=[];
    startToPeak(startToPeak==0)=[];

    if exist('ToFV')==0
        subplot(2,1,1)
        plot(start)
        subplot(2,1,2)
        plot(stop)
        continue
```

```
        end

        % MORE CHECKS
        % if it has less than two peaks - throw it out
        if length(timeConstant)<=2
          continue
        end

        % if there are no recoils - throw it out
        indexOfRecoils = find(earlyOverTotalSmoothed>=.8);
        indexNonRecoils = find(earlyOverTotalSmoothed<.8);
        if length(indexOfRecoils) < 1
            continue
        end

        % if there is only one capture and multiple recoils - throw it out
        if length(indexOfRecoils)>length(indexNonRecoils) && ...
                length(indexNonRecoils)==1
            continue
        end

        % Counter
        nevent=nevent+1;

        % Saving out double capture event data in a structure
        doubleCaptureData(nevent).ToF = ToFV;
        doubleCaptureData(nevent).StartWfm = start;
        doubleCaptureData(nevent).StopWfm = stop;
        doubleCaptureData(nevent).SmoothedStop = stopPolynomial;
        doubleCaptureData(nevent).FirstDerStop = stopFirstDer;
        doubleCaptureData(nevent).SlopePeakIndex = slopePeakIndex;
        doubleCaptureData(nevent).TimeConstant = timeConstant;
        doubleCaptureData(nevent).PeakWidth = peakWidth;
        doubleCaptureData(nevent).PeakIndex = maxAmpOfPeakIndex;
        doubleCaptureData(nevent).EarlyAreaSmoothed = earlyAreaSmoothed;
        doubleCaptureData(nevent).LateAreaSmoothed = lateAreaSmoothed;
        doubleCaptureData(nevent).TotalAreaSmoothed = totalAreaSmoothed;
        doubleCaptureData(nevent).EarlyOverTotalFraction =...
            earlyOverTotalSmoothed;

    end

    % close the waitbar
    waitbar(1,h,'Please Wait...');
    delete(h);

    % add current double capture data to end of last output vector
    doubleCaptureDataOutput = ...
        cat(2, doubleCaptureDataOutput,doubleCaptureData);

end

nValid=length(doubleCaptureDataOutput);
```

```
disp(numOfCaptures)

pause(1) % sometimes uisave does not get called; perhaps this will fix it
uisave({'doubleCaptureDataOutput','dir','nValid'},'doubleCaptureData')
```

Published with MATLAB® R2013a

```
function DoubleCapturePlots(file)
close all
close all hidden

timeConstantV=[];
peakWidthV=[];
peakValueV=[];
earlyAreaSmoothedV=[];
lateAreaSmoothedV=[];
totalAreaSmoothedV=[];
earlyOverTotalSmoothedV=[];
ToFV=[];

for fileNumber = 1:length(file)

    load(char(file));

        % Choose size of final figure
        Units='Centimeters';
        figWidth = 20;
        figHeight = 15.25;
        fig=figure('Units',Units,'Position',[10 10 figWidth figHeight])

    for i=1:nValid
        clear slopePeakIndex peakValue;
        clear peakWidth;
        clear peakIndex;
        clear timeConstant;
        start=doubleCaptureDataOutput(i).StartWfm;
        stop=doubleCaptureDataOutput(i).StopWfm;
        SmoothedStop=doubleCaptureDataOutput(i).SmoothedStop;
        FirstDerStop=doubleCaptureDataOutput(i).FirstDerStop;
        slopePeakIndex=doubleCaptureDataOutput(i).SlopePeakIndex;
        timeConstant=doubleCaptureDataOutput(i).TimeConstant;

        peakWidth=doubleCaptureDataOutput(i).PeakWidth;
        peakIndex=doubleCaptureDataOutput(i).PeakIndex ;
        earlyAreaSmoothed=doubleCaptureDataOutput(i).EarlyAreaSmoothed ;
        lateAreaSmoothed=doubleCaptureDataOutput(i).LateAreaSmoothed ;
        totalAreaSmoothed=doubleCaptureDataOutput(i).TotalAreaSmoothed ;
        earlyOverTotalSmoothed=...
            doubleCaptureDataOutput(i).EarlyOverTotalFraction;
        ToF=doubleCaptureDataOutput(i).ToF;

        x = (1:length(stop))*4/3;

stop=stop/2;
start=start/2;

        subplot(2,1,2)
        plot(x,stop,'k')
        xlab=xlabel('Time (ns)');
```

```
        ylab=ylabel('mV');
        title('Stop Waveform')
        set(xlab,'FontSize',12,'FontName','Arial');
        set(ylab,'FontSize',12,'FontName','Arial');
        axes=gca;
        set(axes,'FontSize',12)

        subplot(2,1,1)
        plot(x,start,'k')
        xlab=xlabel('Time (ns)');
        ylab=ylabel('mV');
        title(['Start Waveform  Event #', num2str(i)])
        set(xlab,'FontSize',12,'FontName','Arial');
        set(ylab,'FontSize',12,'FontName','Arial');
        axes=gca;
        set(axes,'FontSize',12)

        pause

        peakValue=stop(peakIndex);
        peakValue=peakValue';

        timeConstantV = cat(2,timeConstantV,timeConstant);
        peakWidthV = cat(2,peakWidthV,peakWidth);
        peakValueV = cat(2,peakValueV, peakValue);
        earlyAreaSmoothedV=cat(2,earlyAreaSmoothedV, earlyAreaSmoothed);
        lateAreaSmoothedV=cat(2,lateAreaSmoothedV, lateAreaSmoothed);
        totalAreaSmoothedV=cat(2,totalAreaSmoothedV, totalAreaSmoothed);
        earlyOverTotalSmoothedV=cat(2,earlyOverTotalSmoothedV,...
            earlyOverTotalSmoothed);
        ToFV = cat(2,ToFV,ToF);
    end
end
```

Published with MATLAB® R2013a

Bibliography

Adit. 2004, B133D01 Photomultiplier Tube, http://www.aditpmt.com/pmt-datasheets/B133D01W.pdf

Bowman, H. R., Thompson, S. G., Milton, J. C. D., & Swiatecki, W. J. 1962, Physical Review, 126, 2120

Carjan, N., & Rizea, M. 2015, Physics Letters B, 747, 178

Companis, I., Isbasescu, A., Mirea, M., & Petrascu, H. 2010in (EDP Sciences), 1–4

Czirr, J. B. 2016, Private communication

Ellsworth, J. E. 2016, Private communication

ET Enterprises Limited. 2011, Understanding Photomultipliers

Gagarski, A. M., et al. 2008, Bulletin of the Russian Academy of Sciences: Physics, 72, 773

Hamamatsu Photonics K.K. 1999, Hamamatsu Photomultiplier Tube R1250, http://pdf1.alldatasheet.com/datasheet-pdf/view/62677/HAMAMATSU/R1250.html

Kornilov, N. 2015, Fission Neutrons: Experiments, Evaluation, Modeling and Open Problems (Springer), 85

Kornilov, N. V., Kagalenko, A. B., & Hambsch, F. J. 2001a, Physics of Atomic Nuclei, 64, 1373

Kornilov, N. V., Kagalenko, A. B., Poupko, S. V., Androsenko, P. A., & Hambsch, F. J. 2001b, Nuclear Physics A, 686, 187

L'Annunziata, M. F., ed. 2012, Handbook of Radioactivity Analysis, 3rd edn. (Oxford, UK: Elsevier Inc.), 78

Lednicky, R. 2004, Physics of Atomic Nuclei, 67, 72

Lyuboshitz, V. L., & Lyuboshitz, V. V. 2008, Physics of Atomic Nuclei, 71, 454

Martin, R. C., Knauer, J. B., & Balo, P. 1999, in IRRMA '99 4th Topical Meeting on Industrial Radiation and Radioisotope Measurement Applications (Raleigh, North Carolina, October 1999), ed. L. M. E. R. Corp, Chemical Technology Division Oak Ridge National Laboratory (U.S. Department of Energy)

Petrascu, H., Companis, I., Isbasescu, A., & Famiano, M. 2011, Romanian Journal of Physics, 56, 86

Petrov, G. A. 2005in (AIP Publishing), 205–212

Petrov, G. A., et al. 2008, Physics of Atomic Nuclei, 71, 1137

Photogenics. 2008, LGB scintillation crystal for neutron detection

Pringle, J. S., & Brooks, F. D. 1975, Physical Review Letters, 35, 1563

Talou, P., Becker, B., Kawano, T., Chadwick, M. B., & Danon, Y. 2011, Physical Review C, 83, 064612

Wagemans, C., ed. 1991, The Nuclear Fission Process (CRC Press)

Index